nature portfolio

Peer Review File

Cytoplasmic Abundant Heat-Soluble Proteins from Tardigrades Protect Synthetic Cells Under Stress

Corresponding Author: Professor Allen Liu

This file contains all reviewer reports in order by version, followed by all author rebuttals in order by version.

Version 0:

Reviewer comments:

Reviewer #1

(Remarks to the Author)
In the manuscript “Cytoplasmic Abundant Heat-Soluble Proteins from Tardigrades Protect Synthetic Cells Under Stress” the authors test whether CAHS12, a protective disordered proteins from tardigrades, can preserve artificial cells (GUVs as well as the function of several different proteins/enzymes). They look at this protection in the context of short- as well as long-term drying.
While the study of CAHS proteins is of interest and importance, I have several concerns about the manuscript which mostly boil down to two main issues: novelty (and incorporation of prior knowledge) and consistency.

Below I provide more in depth discussion of major and minor concerns, but essentially nearly everything that the authors show in ‘synthetic cells’ as already been shown in prior works – often times in real, living cells. Much of this prior work is simply not discussed or acknowledge and in several cases experimental design in this study has suffered from not taking into account prior knowledge on CAHS proteins. In addition to these issues, the experiments presented in the manuscript do not consistently test the same proteins. Sometimes CAHS12 is used, sometimes CAHS12-GFP is used, sometimes mutants lacking the N or C termini are both used, sometimes only one or the other. There is never any explanation given for why one protein, but not another is used.

Issues/Concerns:

Fig. 1A – the model for CAHS filament formation shown in Figure 1 is out of date, or rather does not take into account what is known about CAHS fibril and gel formation. Work from the Kunieda, Arakawa, Pielak, Boothby, and Blackledge labs have all contributed to our understanding of how CAHS proteins form homotypic interactions. What is displayed in Fig. 1 is not consistent with any of the prior work published on these proteins.

Fig. 1B – What is the timepoint for this experiment? How many cycles were performed? The N and C termini of CAHS proteins as well as the internal linker that bridges these were previously identified and characterized by several groups, but here this is presented as a novel finding. Prior work should be cited.

Fig 1. H and I need a control protein used. What does a protein without any relationship to desiccation tolerance do in these assays? Also, CAHS12-GFP is missing from I, what is the rationale for not including it here when previous experiments used it?

Fig. S1. Several studies previously demonstrated that bacteria expressing CAHS proteins have increased desiccation tolerance, but here this result is presented as novel. Prior work should be acknowledged.

Fig S3. “Surviral rate” has a typo in it. Furthermore, describing something that was never alive as “surviving” does not seem correct to me, please consider changing the working here and elsewhere in the manuscript.

Fig. 2 – Here the necessity of two out of three domains (N and C) was tested, why not test the third domain (linker), especially considering that previous works have identified the linker or subdomains within the linker to be the protective unit of CAHS proteins? Additionally, the authors mention that helix is important for membrane interactions and it is known that the linker is the helical portion of CAHS proteins, so why not look at the helical domain? These experiments test the

necessity of domains for protection, but what about sufficiency? The authors should test these domains in isolation and see if alone they can provide protection.

Fig. 2B – How was prior knowledge from the literature used to guide/test these simulations or the results from them? For example, prior work has suggested that CAHS protein dimerize in an antiparallel fashion, but antiparallel dimerization is not shown in the figure panel.

Fig. 2D – Nothing wrong with this analysis, but this was already known Tanaka et al., and Sanchez-Martinez et al. though no prior credit is given to the authors of these papers for their contributions, rather this result is presented as novel.

Fig. 2E – I think this experiment has a major flaw that is leading to incorrect conclusions. Here, only POPC (which is mostly on the outer leaflet) was used which is a neutral lipid so you would expect to only get hydrophobic residues interact. Why not test with anionic lipids which are on the inner leaflet and so more biologically relevant? The charged, amphipathic linker is more likely to interact with these anionic lipids. Simulating POPC alone is not biologically relevant and I fear this will give readers the wrong impression (that the termini interact with the membrane and the linker does not). Also – I would suggest that the authors examine the literature on LEA proteins (disordered proteins with similarities to CAHS proteins). Particularly looking at work from the Thalhammer lab on LEA protein/membrane interactions would be a good starting point for starting to understand what the field has already determined vis-à-vis desiccation-related IDP/membrane interactions. I think you will see that the linker is the much more likely site of interaction, but that the use of POPC is creating an artefact that shows the opposite.

Fig. 2F what are the percentages displayed here. No text in the figure legend specifying this.

Fig. 3A – Why are different time points shown for CAHS12-GFP and CAHS12deltaN (e.g., 74 vs. 14 days)? Please show matching timepoints to aid in comparison. Also, why are only two of the four proteins used in this study shown here?

Fig. 3B CAHS12-GFP looks so much better than CASH12 alone. Where is the GFP only control?

Fig. 3C – All four proteins tested here, which is great – but leads me to wonder why in A, C, D, E, and F only a subset of the proteins are used.

Fig. 3D Why were different times used for each heating event (not reported for 80C)? Survival rate is not the best term to describe something that was never alive. Where is CAHS12-GFP and deltaC?

Fig. 4 – Broadly, Figure 4 demonstrates in a few different ways that CAHS proteins can protect other proteins/enzymes during drying. This is fine; however many prior studies have shown this and yet the results here are presented as novel. Please give credit to prior works that demonstrated this.

Fig. 4B – mCherry signal already present at 0 hour and then there is still fluorescence after rehydration to me this implies that the signal was there before drying and that you preserved mCherry, not the ability to translate mCherry encoding RNA. A western showing mCherry levels going up after rehydration would show that translation is still happening.

Fig. 4B&J – missing control GUV without CAHS12. E.g., how do we know the transporter breaks when dried?

Fig. 4J – the merge panels are very pixilated please check resolution.

Fig S2 – there are so many degradation bands on this gel. Are the authors purifying these degradation products and using them in their experiments? Also deltaN shows higher order oligomers which contradicts the simulations performed by the authors that suggest fewer interactions between this variant – please explain why there is a discrepancy here.

Fig. S5 – why was BFP used here instead of GFP which is used throughout the rest of the manuscript. I could not find a rationale/justification.

Fig. S6 – Why were different concentrations used for different variants? Please justify.

Fig. S8 Why were no statistics performed here to determine significance? Is the concentration dependence significant?

Fig. S9 – Can the authors comment on why in the fresh GUVs are there so few and large in deltaN?

Fig. S10 – All this has previously been reported, but it is reported here as novel.

Fig. S19 – Prior work has shown that CAHS protein assemblages melt at around 40C. How do the authors imagine protection is taking place at 80C when CAHS assemblages would have been disrupted?

Fig. S20 – It seems from the data that CAHS12-GFP causes GUVs to be very big – this in and of itself is a perturbation. If a cell doubles in size that's not necessarily a good thing. However, this was not observed in live cells in previous works (see Tanaka et al and Sanchez-Martinez et al). Do you think this difference might be an artefact of the GUV system?
What species is this CAHS12 form?

Fig. S1 “Desiccation” spelled “Dessication”

Fig. 1D seems out of place, why is this one panel out of four specifically labeled with “D”? Also C and D in the figure legend seem like they have been mixed up.

(Remarks on code availability)

Reviewer #2

(Remarks to the Author)
The manuscript “Cytoplasmic Abundant Heat-Soluble Proteins from Tardigrades Protect Synthetic Cells Under Stress” by Xi et al. describes a combination of experimental (scanning electron and optical microscopy, interfacial tension measurements) and computational (coarse-grained molecular dynamics simulations) studies of cytoplasmic abundant heat-soluble protein CAHS12, which, among other intrinsically disordered proteins, has been involved in protecting tardigrades from extreme environmental conditions (namely dessication, also elevated temperature, osmotic stress). The importance of this topic far exceeds the understanding of the physiology of these invertebrates, since it may open up exciting technological developments. The manuscript is well organized and clear. The experiments and simulations are well-designed and combine consistently to provide a picture that, under dessication, CAHS12 undergoes a reversible structural transformation (oligomerizes in a filamentous network, within the lumen of cell membrane-mimicking vesicles) that reinforces membrane integrity and protection, thus providing important new insights. I have the following minor comments:
1) Page 5 in the pdf file (no page numbers are actually provided): “Over the concentration range of 0.1–1.0 mM, CAHS12 exhibited a modest increase in interfacial tension (from ~12 to ~15 mN/m) (…) In contrast, the ΔN variant showed a more pronounced increase in IFT over the same range (from ~6 to ~8 mN/m)”. As the numbers (and indeed the plots in Fig. 1I) show, the absolute IFT increase for the ΔN variant is not more pronounced than that for CAHS12.
2) Page 21: “upper and lower boundaries of the lipid headgroup region” – these boundaries may have been defined from the z positions of adequate CG beads, please explain in more detail.
3) Page 31, legend of Fig. 1A: “CAHS12 disassembles from the membrane interface, releasing tension and allowing fluidity of lipids on the membrane (…)” – actually the part about membrane order/fluidity has not been validated from this study, although the MD simulations could provide an adequate test, which the authors should consider doing.

(Remarks on code availability)
The authors have provided simulation setups, scripts, and analyses related to this study. Although no trajectories are made available, the provided files constitute useful resources for someone willing to take inspiration for new work.

Reviewer #3

(Remarks to the Author)
This manuscript by Xi et al. not only confirms the protective role of CAHS12 on GUV phospholipid membranes during dehydration-rehydration cycles but also precisely identifies its N-terminal disordered region as the critical functional domain. Furthermore, it successfully demonstrates the ability to preserve the functionality of both cell-free transcription-translation (CFE) systems encapsulated within GUVs and membrane proteins incorporated into the phospholipid bilayer under long-term dry storage. This manuscript provides an interesting method to maintain the artificial cell stability. I would like to recommend it for publication after addressing below points.

1. Figure 1G shows the redistribution of CAHS12-GFP during the rehydration process. Would it be possible to monitor the distribution changes of CAHS12-GFP a during the dehydration and rehydration process? How many cycles do those artificial cells undergo dehydration-rehydration?
2. In Figure 1I, the three data points for the three proteins at 0 mM concentration, and the point at 0 on the protein-free curve, should represent identical conditions. Why is there a significant variation in the measured tension among these four points?
3. In the long-term CFE preservation experiment, a crucial quantitative control is missing. How much activity, if any, is retained by the CFE system in solution (not encapsulated within GUVs) under the same desiccation conditions? This would more clearly delineate the respective contributions of GUV encapsulation versus CAHS12 protection.
4. Regarding the definition of "survival rate," how is the survival rate of GUVs precisely defined? Is it based solely on morphological integrity, content retention, or a combination of both?
5. Molecular simulations strongly suggest that CAHS12 forms a filamentous network upon dehydration. Is there any more direct experimental evidence, or reported by literature?

(Remarks on code availability)

Version 1:

Reviewer comments:

Reviewer #1

(Remarks to the Author)
The authors have systematically addressed all my major/minor concerns. With these revisions and explanations I find what was already an interesting paper even more compelling. I have no further concerns and would like to extend my thanks to the authors for their extensive revisions and addressing everything I had questions about. This is a really interesting and informative study. Well done!

(Remarks on code availability)

Reviewer #2

(Remarks to the Author)
The authors have answered my comments adequately and carried out the corresponding required changes. I have no further comments.

(Remarks on code availability)
As I previously pointed out, the authors have provided simulation setups, scripts, and analyses related to this study. Files pertinent to the new simulations carried out during revision have now been added.

Reviewer #3

(Remarks to the Author)
The authors well addressed my comments. It can be published in its present form.

(Remarks on code availability)

Response to the reviewers' comments

We thank the reviewers for their time and dedication invested in reviewing our manuscript. In light of their feedback, we have carefully addressed and responded to the points raised in the reviewers' comments. Our detailed responses to each point can be found written in blue following the respective comments. The text added to the manuscript in response to the reviewer's comments is in red. We appreciate your involvement with our work. Your constructive criticism is greatly valued, as it enhances the quality of this manuscript.

Reviewer #1 (Remarks to the Author)

In the manuscript "Cytoplasmic Abundant Heat-Soluble Proteins from Tardigrades Protect Synthetic Cells Under Stress" the authors test whether CAHS12, a protective disordered proteins from tardigrades, can preserve artificial cells (GUVs as well as the function of several different proteins/enzymes). They look at this protection in the context of short- as well as long-term drying. While the study of CAHS proteins is of interest and importance, I have several concerns about the manuscript which mostly boil down to two main issues: novelty (and incorporation of prior knowledge) and consistency.

Below I provide more in depth discussion of major and minor concerns, but essentially nearly everything that the authors show in 'synthetic cells' as already been shown in prior works – often times in real, living cells. Much of this prior work is simply not discussed or acknowledge and in several cases experimental design in this study has suffered from not taking into account prior knowledge on CAHS proteins. In addition to these issues, the experiments presented in the manuscript do not consistently test the same proteins. Sometimes CAHS12 is used, sometimes CAHS12-GFP is used, sometimes mutants lacking the N or C termini are both used, sometimes only one or the other. There is never any explanation given for why one protein, but not another is used.

Response: We thank the reviewer for the thoughtful comments. We have revised the manuscript substantially to address concerns regarding (i) novelty and incorporation of prior literature, and (ii) consistency and justification of the protein constructs used.

We agree that earlier studies demonstrated that CAHS proteins confer mechanical and desiccation protection in living cells and in vitro. We now explicitly discuss these foundational studies, particularly from the Tanaka[1] group and the Boothby[2] group, and clearly delineate how our study extends these findings by demonstrating: (i) Protection of synthetic membrane-bound compartments (GUVs) under both rapid and long-term desiccation. (ii) Formation of CAHS

networks inside GUVs, including domain-dependent assembly not previously observed in confined synthetic compartments. (iii) Recovery of synthetic-cell biochemical function (i.e., cell-free expression) after drying, which represents a distinct application-oriented demonstration beyond earlier cellular studies.

We added a dedicated paragraph in the Introduction and Discussion summarizing prior findings and clarifying the conceptual gap our study fills.

Revised Introduction:

'… While classical models emphasize osmolytes like trehalose or antioxidants[3], growing evidence implicates a family of tardigrade intrinsically disordered proteins, namely the cytoplasmic-abundant heat-soluble (CAHS) proteins, as the primary drivers of this exceptional dry-state tolerance[3].

*Tardigrades possess a diverse repertoire of cytoplasmic abundant heat-soluble (CAHS) proteins with partially overlapping yet isoform-specific functions under stress. Under hydrated conditions, CAHS proteins are largely unstructured; upon dehydration or osmotic stress, they undergo reversible, stress-responsive conformational transitions, with intrinsically disordered N- and C-terminal regions flanking a central α-helical linker domain (Fig. 1A). Early biochemical and biophysical studies demonstrated that CAHS proteins can vitrify and suppress protein aggregation under water loss, implicating them as molecular stabilizers during anhydrobiosis[2,4]. Complementary work showed that CAHS proteins form gel-like or filamentous assemblies in vitro and in cells under dehydration or crowding, and that these assemblies correlate with enhanced mechanical resilience and cellular survival (**Supplementary Fig. 1**)[1,5,6].*

High-resolution structural and spectroscopic studies further refined this view by revealing that CAHS proteins remain highly dynamic and only partially ordered even within stress-induced assemblies. In particular, NMR and scattering analyses from the Blackledge laboratory demonstrated that CAHS proteins form adaptable, weakly interacting networks rather than rigid scaffolds, supporting a model of emergent protection driven by multivalent, reversible interactions[7]. More recently, cellular imaging and genetic perturbation studies showed that CAHS proteins reversibly reorganize into filamentous networks during dehydration and rapidly dissolve upon rehydration without compromising mammalian cell viability, reinforcing their role as stress-responsive biomolecular materials rather than static structural elements[6].

Despite these advances, prior studies have largely focused on molecular assembly, material properties, or organismal survival. Whether CAHS proteins can preserve functional biochemical

activity, particularly over extended periods of dry storage, has not been directly tested. Moreover, most demonstrations to date have been conducted in living cells or complex extracts, where endogenous repair pathways, chaperones, and metabolic processes obscure the individual contributions of CAHS-mediated membrane stabilization and protein protection.

Here, we focus on CAHS12, a conserved and abundantly expressed CAHS isoform induced during desiccation, previously shown to form reversible filamentous assemblies under stress[1]. To isolate the mechanism from cellular complexity, we reconstituted CAHS12 and its truncation variants within giant unilamellar vesicles (GUVs) as a minimal synthetic cell platform. This reductionist system enables direct interrogation of CAHS-mediated membrane stabilization and long-term functional preservation under dehydration. Notably, we demonstrate that CAHS12 enables sustained preservation of cell-free transcription–translation activity and membrane protein function within dehydrated GUVs, extending prior structural and cellular observations to long-term functional protection in synthetic cells.'

Revised discussion:

'…indicating that CAHS12 enables functional preservation of encapsulated proteins under extreme drying stress. Prior studies have established that CAHS proteins can act as protein stabilizers during drying, preserving enzymatic activity in vitro[2,8]. Our results confirm and extend these findings by demonstrating that sequence-based variants of CAHS differ in their efficacy across client molecules and environmental conditions, suggesting mechanisms by which intrinsic disorder and phase behavior tune desiccation protection.'

We acknowledge that the original manuscript did not sufficiently explain why CAHS12, CAHS12-GFP, and truncation mutants were used in different experiments. We have now added a clear justification:

Fluorescently tagged CAHS12 (GFP or BFP) was used to image CAHS localization and assembly in GUVs. In addition to imaging, fluorescently tagged CAHS12 served as an independent fluorescent control to assess whether tagging affects CAHS12-mediated GUV protection. N- and C-terminal truncation mutants (ΔN, ΔC) were used to probe domain-specific contributions to assembly and protection. All figure legends specify the construct used; assignments are summarized in **Supplementary Table 7**.

Supplementary Table 7. *Assignment of CAHS12 constructs to experimental assays*

CAHS12 construct	***Tag***	***Primary purpose***	***Assays used***

CAHS12 (full length)	*None*	*Functional protection without tag interference*	*Long-term dry storage assays; interfacial tension measurements; thermal stability*
CAHS12–GFP	*GFP*	*Visualization of protein localization and assembly*	*Confocal imaging of GUVs; dehydration–rehydration dynamics; network formation; interfacial tension measurements; thermal stability*
CAHS12–BFP	*BFP*	*Visualization of protein localization and assembly*	*Confocal imaging of GUVs; Control to test tag effects on GUV protection*
CAHS12 ΔN	*None*	*Dissection of role of N-terminal region*	*GUV protection assays; interfacial tension measurements; stability comparisons*
CAHS12 ΔC	*None*	*Dissection of role of C-terminal region*	*GUV protection assays; interfacial tension measurements; stability comparisons*

Issues/Concerns:

1. Fig. 1A – the model for CAHS filament formation shown in Figure 1 is out of date, or rather does not take into account what is known about CAHS fibril and gel formation. Work from the Kunieda, Arakawa, Pielak, Boothby, and Blackledge labs have all contributed to our understanding of how CAHS proteins form homotypic interactions. What is displayed in Fig. 1 is not consistent with any of the prior work published on these proteins.

Response: We thank the reviewer for highlighting the need to align our model with current understanding of CAHS protein assembly. We have updated **Fig. 1A** to reflect the reversible sol–gel transition of CAHS12 and its dehydration-induced formation of a filamentous/gel-like network within vesicles. This network buffers membrane deformation without protein insertion, consistent with prior work[1,2,6,7,9].

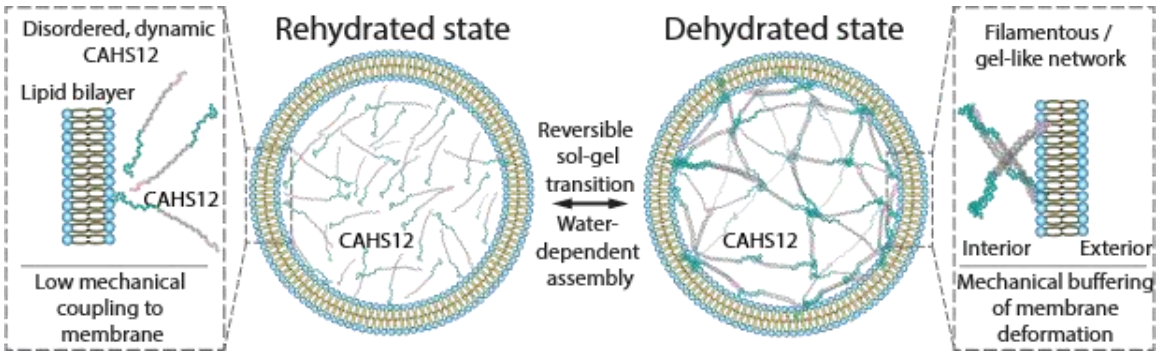

Fig. 1. (A) Updated mechanistic model of CAHS12-mediated protection. *Under hydrated conditions, CAHS12 remains highly disordered and dynamically distributed within GUVs, exhibiting transient homotypic interactions. Upon dehydration, reduced water activity*

induces reversible CAHS12 self-association into an extended filamentous or gel-like network within the vesicle lumen. This network mechanically couples to the confined volume and buffers membrane deformation without requiring stable membrane insertion. Rehydration restores the disordered, sol-like state. This model is consistent with prior reports of dehydration-induced CAHS gelation and filament formation.

2. Fig. 1B – What is the timepoint for this experiment? How many cycles were performed? The N and C termini of CAHS proteins as well as the internal linker that bridges these were previously identified and characterized by several groups, but here this is presented as a novel finding. Prior work should be cited.

Response: We appreciate the reviewer's careful inspection of **Fig. 1B**. We have revised the manuscript to clarify the experimental details.

We now specify in the Results and Methods that **Fig. 1B** corresponds to **a** single dehydration–rehydration cycle, imaged within 10 minutes after rehydration. We further note that identical trends were observed after three consecutive cycles, now reported in a new Supplementary Figure (**Supplementary Fig. 3A**).

We fully agree that the N/C termini and the central linker of CAHS proteins have been defined and biophysically characterized in previous work[1,5,6,10]. We did not intend to present the domain architecture as a novel discovery. Instead, our contribution is to test how these established domains behave inside a confined vesicle environment (i.e., GUVs) during drying/rehydration.

To address these comments, we introduced the following changes in the revised manuscript.

- In the Introduction, we now explicitly cite the foundational studies that characterized CAHS termini, linker disorder, helix-forming propensity, and assembly behavior.
- In the description of **Fig. 1B**, we revised wording to make clear that the domain boundaries are **not** newly identified here; our novelty lies in testing domain-dependent intraluminal network formation and protective function inside synthetic cells.
- Added relevant citations to all domain references, including Tanaka, Akihiro, *et al. PLoS Biology* (2022); Sanchez‐Martinez, S., *et al. Protein Science* (2024); Yagi-Utsumi, Maho, *et al. Scientific Reports* (2021). Biswas, Sourav, *et al. Protein Science* (2024)[1,5,6,10].

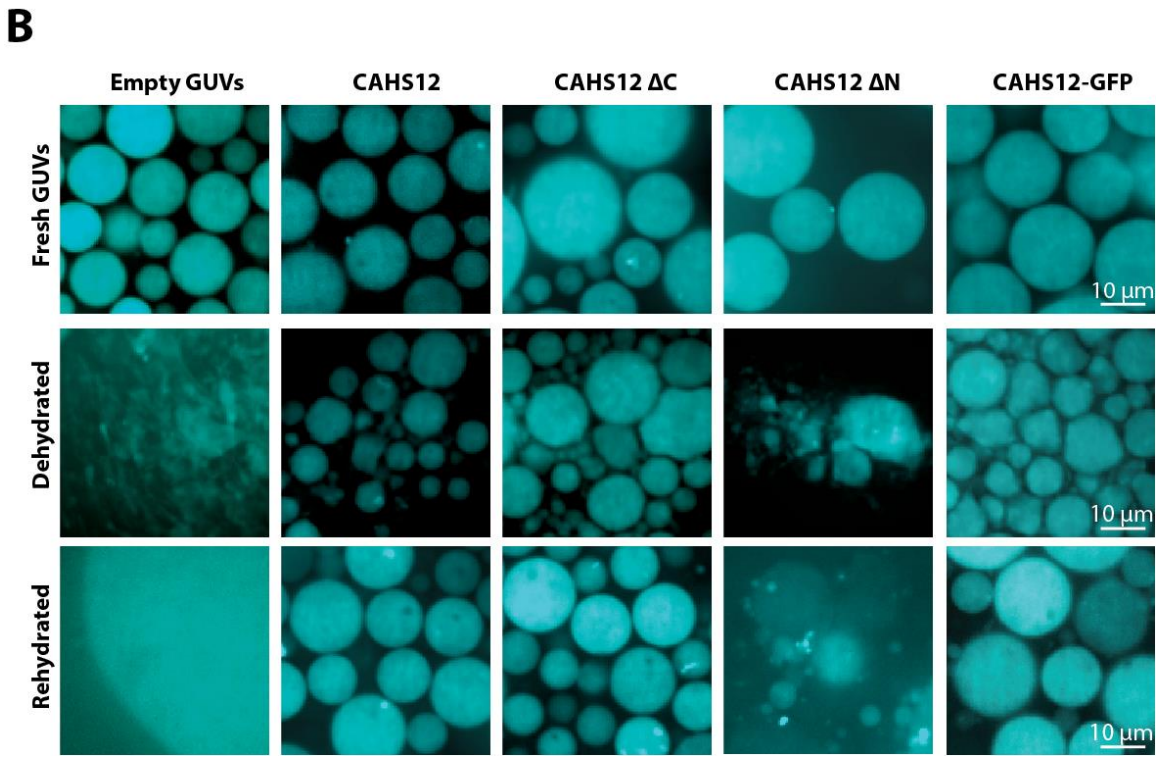

Fig. 1. *(**B**) Fluorescence microscopy images of CAHS12-loaded GUVs under fresh, dehydrated, and rehydrated states. Cy5 encapsulated within the GUV lumen was used as a leakage reporter to assess membrane integrity based on its release. The CAHS12 domain architecture shown is based on previous studies, and the experiments here examine how these domains contribute to intraluminal assembly and protection of GUV membranes.*

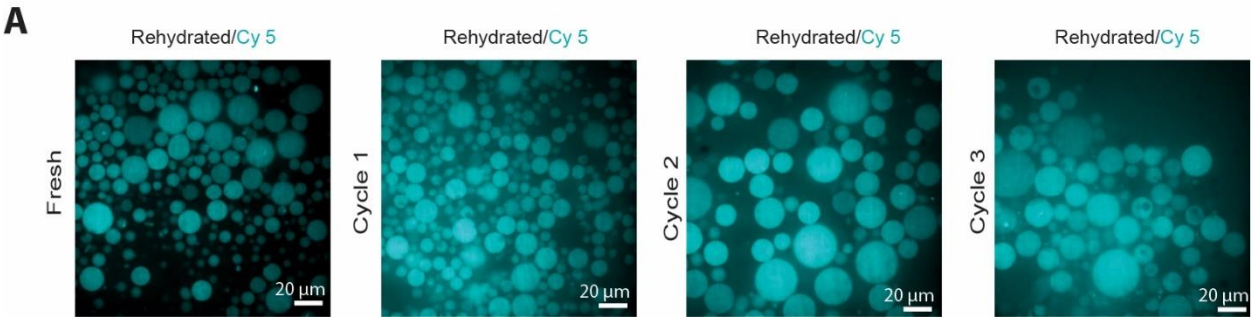

Supplementary Fig. 3A. Representative fluorescence microscopy images of GUVs after repeated dehydration–rehydration cycles. *Representative fluorescence microscopy images of GUVs following three consecutive dehydration–rehydration cycles. After each dehydration step (vacuum desiccation at ~31 mbar for ⩾12 h), samples were rehydrated by adding ultrapure water and incubated at room temperature for 10 min to allow complete rehydration before imaging or the initiation of the subsequent cycle. Vesicle morphology and integrity were assessed after each*

rehydration. Some vesicles appeared larger after the second dehydration–rehydration cycle, for reasons we do not fully understand.

3. Fig 1. H and I need a control protein used. What does a protein without any relationship to desiccation tolerance do in these assays? Also, CAHS12-GFP is missing from I, what is the rationale for not including it here when previous experiments used it?

Response: We thank the reviewer for this important suggestion. In accordance with the comment, we have now added a non-desiccation-related protein, BSA, as a control condition to **Supplementary Fig. 8C.** This protein was tested at the same concentration and under identical buffer conditions as CAHS12. We found that BSA behaved similarly to the buffer-only group with negligible interfacial adsorption. In contrast, CAHS12 and its variants exhibited robust interfacial activity. These control experiments confirm that the protective effects are specific to CAHS12 rather than arising from generic protein crowding.

Regarding the absence of CAHS12-GFP in **Fig.1I.**, we have now included CAHS12-GFP in the updated panel. The CAHS12-GFP fusion displayed protection equivalent to untagged CAHS12, consistent with the results shown earlier in the manuscript. This confirms that the GFP tag does not alter the protective activity of CAHS12. Corresponding descriptions have been incorporated into the figure legend and Methods section.

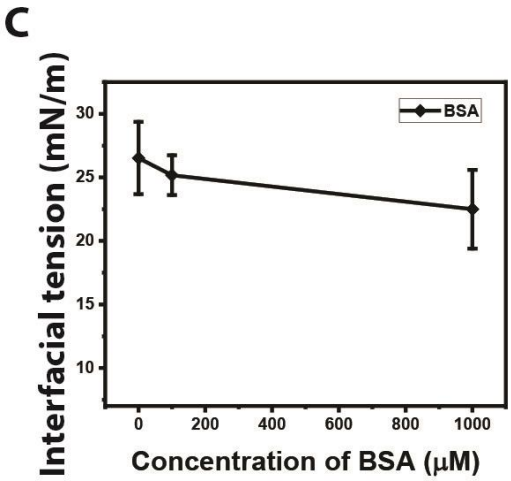

Supplementary Fig. 8. **(C)** IFT as a function of concentration for BSA.

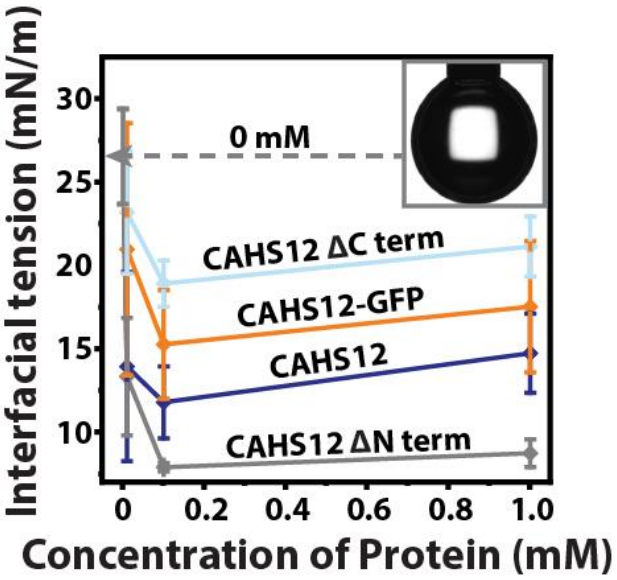

Fig. 1. (**I**) IFT as a function of concentration for CAHS12, CAHS12-GFP, CAHS12 ΔC, and CAHS12 ΔN. Inset shows the morphology of a pure water droplet suspended in mineral oil containing 0.41 mM POPC.

4. Fig. S1. Several studies previously demonstrated that bacteria expressing CAHS proteins have increased desiccation tolerance, but here this result is presented as novel. Prior work should be acknowledged.

Response: We thank the reviewer for pointing this out. We fully agree that prior studies have shown that heterologous expression of CAHS proteins can increase bacterial desiccation tolerance[1,5,6,11]. Our intention was not to present this result as novel. In the revised manuscript, we now explicitly acknowledge this prior work in both the main text and the **Supplementary Fig. 1** legend. We clarify that the purpose of including this experiment is to confirm that our CAHS12 construct behaves as expected in a well-established biological context, thereby validating the protein preparations used in our synthetic cell experiments. The revised text now states clearly that this result is a reproduction of previously reported phenomena, included for experimental completeness, hence as a supplementary figure, rather than novelty.

*'Previous studies showed that CAHS proteins form gel-like or filamentous assemblies in vitro and in cells under dehydration or crowding, and that these assemblies correlate with enhanced mechanical resilience and cellular survival (**Supplementary Fig. 1**)[1,5,6]'*

'Supplementary Fig. 1. *(**C**) Colony formation assay showing viability of E. coli expressing CAHS12-GFP after desiccation under ambient conditions (top) and vacuum (bottom). Plates on the left show wildtype E. coli after 4 days of desiccation, with minimal colony formation. Plates on the right show cells expressing CAHS12-GFP after 6 days of desiccation before plating, exhibiting robust colony recovery under both ambient and vacuum conditions. This result is consistent with prior studies reporting increased bacterial desiccation tolerance upon heterologous expression of CAHS-family proteins[1,2,5]. Scale bar, 1 cm.'*

5. Fig S3. "Surviral rate" has a typo in it. Furthermore, describing something that was never alive as "surviving" does not seem correct to me, please consider changing the wording here and elsewhere in the manuscript.

Response: We thank the reviewer for this helpful comment. We agree that describing synthetic cells as "surviving" is misleading, as they are not living systems. Throughout the revised manuscript—including **Supplementary Fig. 3**, figure legends, and Results text—we have replaced this terminology with more accurate descriptors such as "retention rate" or "dye retention". This revision ensures the language reflects the non-living nature of the system and avoids unintended biological implications.

6. Fig. 2 – Here the necessity of two out of three domains (N and C) was tested, why not test the third domain (linker), especially considering that previous works have identified the linker or subdomains within the linker to be the protective unit of CAHS proteins? Additionally, the authors mention that helix is important for membrane interactions and it is known that the linker is the helical portion of CAHS proteins, so why not look at the helical domain? These experiments test the necessity of domains for protection, but what about sufficiency? The authors should test these domains in isolation and see if alone they can provide protection.

Response: We thank the reviewer for this insightful suggestion and agree that the linker domain has been implicated in the protective function of CAHS proteins in prior studies[10]. In our current experimental and simulation framework, the truncation studies were designed to probe domain necessity within the context of vesicle protection and in the regime of the tested conditions. We find that removal of the N-terminal region (ΔN) already abolishes the protection of POPC vesicles under our assay conditions. Given this significant loss of activity, further ablation of the C-terminal domain, which results in a linker-only structure, is likely to yield equal or worse performance in this specific context.

To directly assess the plausibility of linker-only protection, we performed additional coarse-grained molecular dynamics simulations of the linker domain interacting with a POPC membrane. In contrast to the full-length CAHS 12 that forms percolated networks, the linker-only construct shows predominantly dispersed monomers or short filament-like structures. Additionally, protein-membrane contacts are sparse, which suggests weak association with POPC bilayers and a lack of cooperative membrane engagement (**Fig. 2C** and **Fig. 2D**, **Supplementary Fig. 14**). We emphasize that these results are specific to POPC membranes and are interpreted within the context of synthetic cell applications, where POPC is prevalently used as a minimal and well-defined membrane system. We show in another response to the reviewer's question that the interaction profiles of linkers with lipid membranes are sensitive to membrane compositions. Our goal here is not to recapitulate the full biological complexity of CAHS-membrane interactions in a biological setting but to evaluate functional protection in a controlled synthetic condition for POPC-based lipid membranes.

Consistent with our observations, prior experimental works have shown that the linker domain alone, or isolated terminal regions, exhibit substantially reduced protective capacity compared to full-length CAHS proteins in enzyme stabilization assays (e.g., LDH protection)[1,10,12]. These results indicate that the linker alone does not produce the same level of protection provided by full-length CAHS proteins under matched conditions. However, studies have reported that isolated linker or truncated constructs can exhibit partial protective activity in enzyme stabilization assays when used at higher concentrations than full-length CAHS proteins[10], exposing a concentration-dependent form of sufficiency.

We again thank the reviewer for raising these important questions and have revised the manuscript to include simulation results for the linker-only systems. In the Results section in the main text, along with a commensurate augmentation of **Fig. 2**. The simulation input files and data have been updated to the GitHub Repository at https://github.com/Ferg-Lab/CAHS-Protein-Simulations.

*'To further dissect the roles of each terminal region in CAHS12 assemblies, we constructed ΔC, ΔN, and ΔCΔN variants by truncating the respective regions while preserving the conformation of the remaining protein (**Supplementary Fig. 15**, **Supplementary Table 1, 4, 5, 6**). Network analyses of multimer simulations with POPC membranes show that both the wild-type CAHS12 and the ΔC variant form protein networks and filaments (**Fig. 2C** and Supplementary Fig. 14) with comparable cluster numbers, sizes, and node connectivity (**Fig. 2D**). In contrast, the ΔN variant exhibits a significantly reduced capacity to form networks (**Fig. 2C** and **Supplementary***

*Fig. 16), with increased cluster numbers and decreased cluster sizes and connectivity (**Fig. 2D**). The ΔCΔN variant leaving just the linker region leads to a further decrease in capacity to form interconnected assemblies.'*

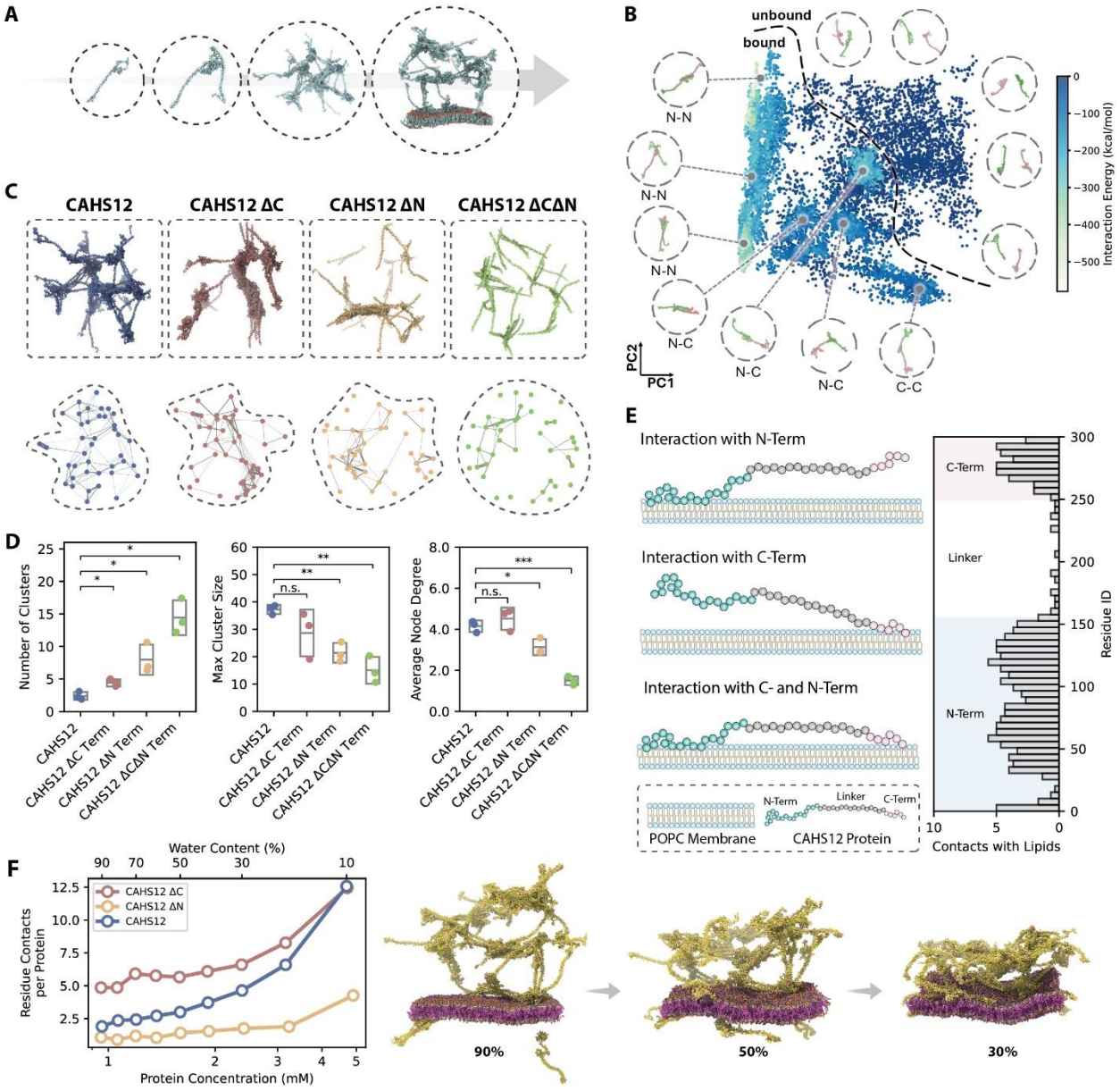

Fig. 2. Molecular dynamics simulations of CAHS12 protein assemblies and their interaction with phospholipid membranes. (A) Schematic depiction of the simulation systems with increasing structural complexity, ranging from a single CAHS12 monomer (left) to oligomers, fibrillar networks, and large-scale assemblies interacting with a POPC lipid membrane (right). (B) A PCA plot of CAHS12 dimer conformations from unbiased simulations presenting representative dimer configurations from selected clusters. The color scale indicates interaction strength based on short-range inter-protein interaction energy. The dashed line approximately delineates the bound

and unbound states. (C) Network representations of protein assemblies for wild-type CAHS12, ΔC, ΔN, and ΔCΔN variants. Nodes represent individual proteins; edges represent the contact among proteins; edge thickness is proportional to the inverse of the center-of-mass distance between two proteins. (D) Quantification of differences in topological organization between the CAHS12, CAHS12 ΔC, CAHS12 ΔN, and CAHS12 ΔCΔN variants for the systems shown in (C). The number of clusters represents the count of distinct and connected protein assemblies. The maximum cluster size denotes the largest number of proteins within a single connected cluster. The average node degree indicates the mean connectivity per protein. The box bounds represent standard deviations from three independent replicates, and the middle lines represent the mean. Statistical significance was assessed using Welch's t-test. (E) Schematic models of membrane-binding modes for the CAHS12 protein, illustrating the interaction between different domains of the protein, particularly the C- and N-terminal domains, with the POPC membrane (left). Contact frequency of residues across the whole CAHS12 sequence supporting the proposed models (right). Contacts are quantified by identifying residues within 0.5 nm of POPC lipid headgroups and averaging the counts over simulation frames. (F) Residue-level membrane contact analysis for CAHS12, CAHS12 ΔC, and CAHS12 ΔN during progressive water removal simulations (i.e., increasing protein concentration), along with the molecular visualization showing the CAHS12 protein and POPC membrane, mimicking the desiccation process. The percentage indicates the fraction of remaining water beads relative to the initial simulation box, with a lower value corresponding to a greater extent of water removal. Contacts are defined as the number of unique residues that are within 0.5 nm of POPC lipid headgroups, normalized by the number of CAHS12 proteins. All data in (C-F) were collected from the final 500 ns of the 1500 ns simulations. Statistical analyses were performed on averaged data points from three independent simulations. A Welch's t-test (two-tailed) between CASH12 and CAHS12 ΔC or CAHS12 ΔN was used in (D) to assess statistical significance. *, $p < 0.05$; **, $p < 0.01$.

In the Methods section, we modified the simulation protocol accordingly.

*'… Additionally, we included the ΔC, ΔN, and ΔCΔN variants lacking, respectively, the C terminal domain, N terminal domain, and C and N terminal domains to assess the respective contributions of the terminal regions to membrane association and network formation (**Supplementary Fig. 15**, **Supplementary Tables 1, 4, 5, 6**). …'*

'… Subsequently, in 3 separate simulations, 40 wildtype CAHS12 proteins, ΔC, ΔN, and ΔCΔN variants were randomly introduced into the bulk water above the membrane. …'

'… Each system was prepared and simulated in three independent replicates leading, to a total of 12 simulations. …'

In addition, the sequence of the ΔCΔN variants was added to **Supplementary Table 6**, and the corresponding **Supplementary Fig. 15** and **Supplementary Fig. S16** were updated.

Supplementary Table 6 *Sequence of CAHS12 ΔCΔN*

AEAREKRMRDEEKYAREQEAINRHADKDLEKKTEAYRKEAEHEAEKIRKALEKQHERDIEFR KEVVGSTIEKQKAEIELEAKRAKAALEHERQLANDALERSKMHTDVQVTMDT

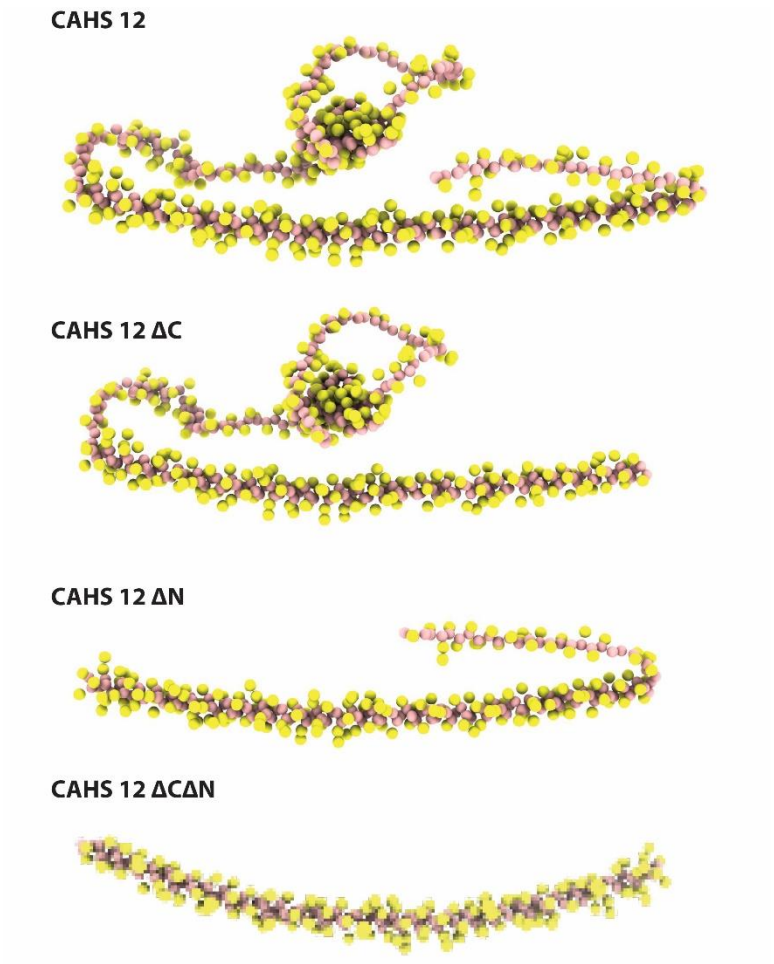

Supplementary Fig. 15. Coarse-grained models of the CAHS12 protein and its terminal truncation variants (CAHS12 ΔC, CAHS12 ΔN, and CAHS12 ΔCΔN). The pink

beads represent protein backbone while yellow beads represent side chains of residues. The models illustrate the overall architecture of the wild-type and truncated proteins used in simulations. Secondary structures were predicted using AlphaFold 3 and assigned during coarse graining using define secondary structure of proteins (DSSP) algorithm. The structures were visualized by ChimeraX.

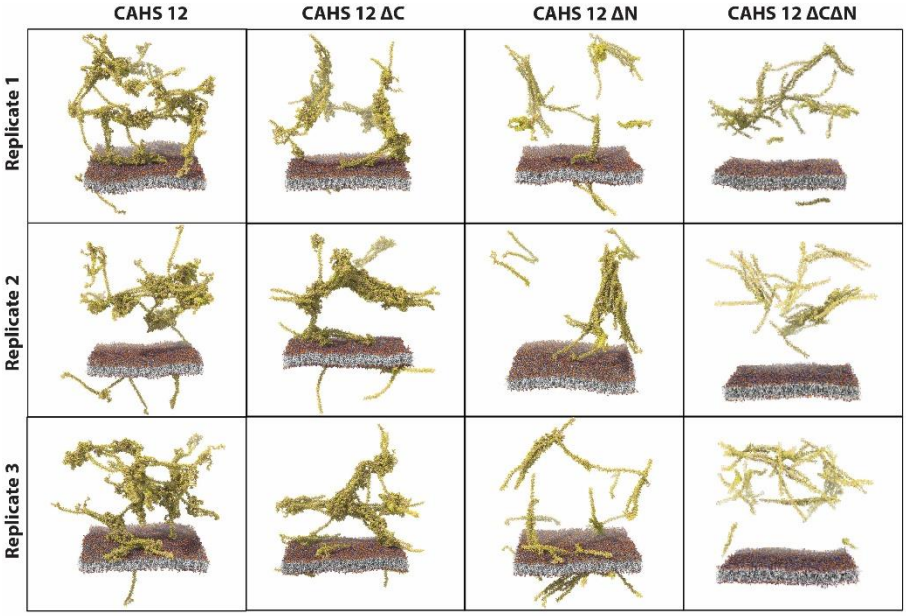

Supplementary Fig. 16. Simulations of CAHS12 proteins and POPC membranes. Final snapshots from each simulation were visualized using ChimeraX. Three independent replicates were performed for each system, all of which yielded consistent phenomenological observations regarding protein assembly and membrane association.

7. Fig. 2B – How was prior knowledge from the literature used to guide/test these simulations or the results from them? For example, prior work has suggested that CAHS protein dimerize in an antiparallel fashion, but antiparallel dimerization is not shown in the figure panel. **Response:** We greatly appreciate the reviewer's comment and agree that the inclusion of prior knowledge from the literature can further inform the interpretation of the dimer interactions shown in **Fig. 2B**. We have therefore revised the main text to more explicitly describe how previous reports of CAHS dimerization, including antiparallel arrangements, were considered in interpreting the results.

With regard to the dimerization conformations, **Fig. 2B** summarizes the binding configurations observed in unbiased simulations initiated from randomly placed CAHS12

monomers separated in a simulation box. Following these simulations, we conducted four additional independent unbiased simulations using the same protocol and still failed to observe the antiparallel binding event. The low frequency of observing this configuration may, however, be due to the fact that the antiparallel conformation is kinetically less accessible than other binding modes on the time scales simulated here, rather than an intrinsically lower thermodynamic stability.

Therefore, to directly probe the thermodynamic stabilities without kinetic accessibility concerns, we performed free energy calculations in which the two CAHS12 proteins were explicitly initialized in parallel or antiparallel configurations obtained by manual placement, and their relative dissociation behavior was examined using umbrella sampling. These calculations required a substantially larger simulation box (50 nm) and more than 50 umbrella windows per system, leading to markedly increased computational cost. As shown in **Supplementary Fig. 13**, the antiparallel configuration exhibits a higher dissociation free energy than the parallel configuration, which suggests that the antiparallel dimer is more thermodynamically stable than the parallel dimer. This trend is consistent with the reviewer's comment and prior reports in which the antiparallel CAHS12 dimer structure was proposed by most models, including AlphaFold2.

The predictions of AlphaFold2 and other protein structure prediction tools focus on the most stable configuration without consideration of metastable states, ensembles of configurations, or kinetic assembly pathways and mechanisms. Molecular dynamics simulations explicitly probe the mechanism of dimerization from the separated monomers. As such, the difference between the free energy trend and the failure of spontaneous antiparallel dimerization from unbiased simulations does not imply a contradiction but instead suggests that kinetic accessibility and thermodynamic stability appear to play competing roles under the simulation conditions considered here. In this context, **Fig. 2B** is intended to highlight the potential interaction modes observed in unbiased simulations, particularly the role of terminal-region interactions that may contribute to the network assembly.

Finally, we emphasize that multiple binding poses, including both parallel and antiparallel arrangements proposed in the literature, are likely relevant and may collectively contribute to the formation of higher-order network or filamentous assemblies of CAHS12 proteins. In more realistic settings involving many interacting proteins and complex environments, as opposed to an isolated dimer, a diverse range of conformations is expected to coexist.

To clarify these points and include prior knowledge, we have added a discussion in the Results section that places the results shown in **Fig. 2B** in the context of prior work on antiparallel dimerization, and we have also updated our revised manuscript to incorporate the additional

unbiased simulations and report our free energy calculations. The corresponding changes are reproduced below.

*'… C-terminal-only interactions, as measured by the short-range inter-protein interaction energy. We note that antiparallel CAHS12 dimer conformations have been predicted in prior studies using structure prediction tools[5]. Free energy calculations indicate that the antiparallel dimer is approximately 20 kcal/mol more stable than the parallel dimer (**Supplementary Fig. 13**), but we observe only the parallel dimer state in our unbiased calculations and no significant population of the antiparallel dimer. This suggests that while the antiparallel dimer may be more thermodynamically stable, it may be less kinetically accessible than the parallel dimer state. Furthermore, a large proportion of the observed dimers do interact via binding between the C- and N-terminal regions that may be precursors to antiparallel dimers in longer simulations[1,7,13].'*

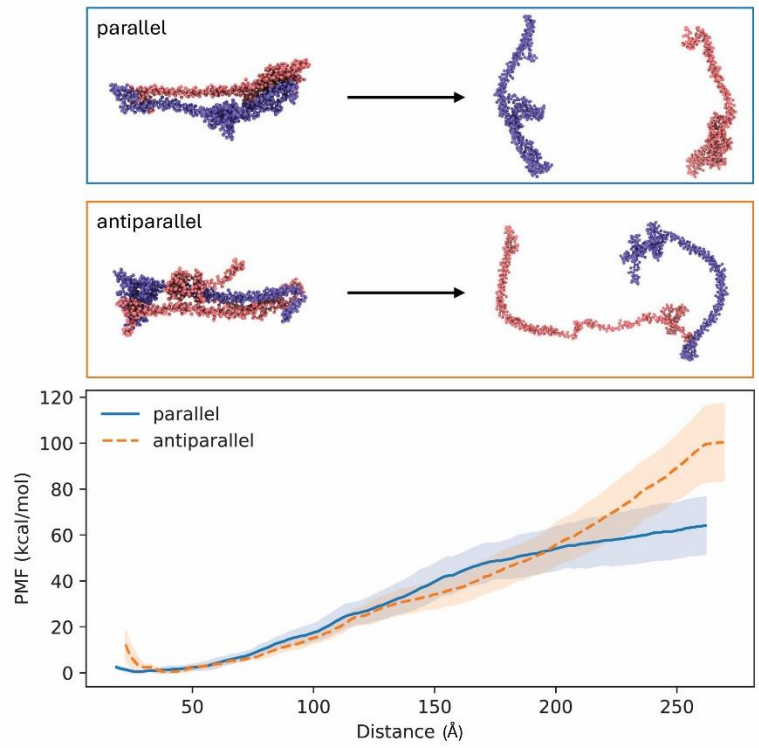

Supplementary Fig. 13. Free energy calculations of dissociation of CAHS dimers from parallel and antiparallel conformations. The upper panel shows representative initial bound structures and the corresponding final dissociated states. The lower panel reports the free energy profiles along the dissociation coordinate. Fifty window simulations with an interval of 0.5 nm were extracted and simulated using GROMACS and PLUMED[14]. The free energy profiles were

computed using WHAM from the final 20 ns simulations[15]. The shaded areas present the uncertainty of the free energy profiles obtained from four-fold block analysis.

Fig. 2B, along with its corresponding **Supplementary Fig. 12** are shown below to include additional independent simulations.

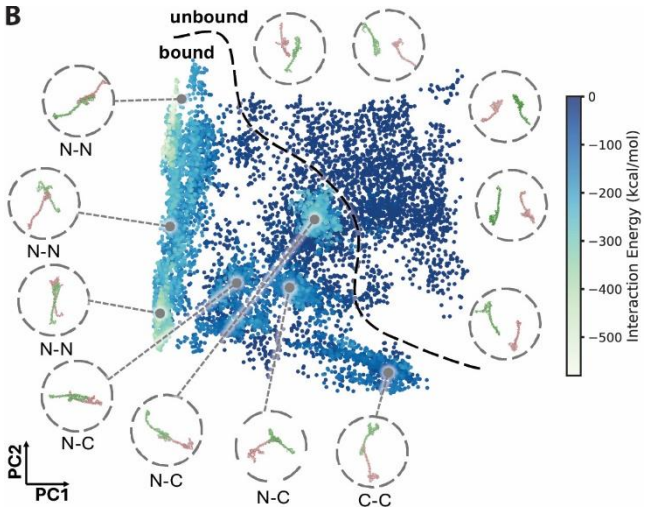

Fig. 2. (**B**) A PCA plot of CAHS12 dimer conformations from unbiased simulations presenting representative dimer configurations from selected clusters. The color scale indicates interaction strength based on short-range inter-protein interaction energy. The dashed line approximately delineates the bound and unbound states.

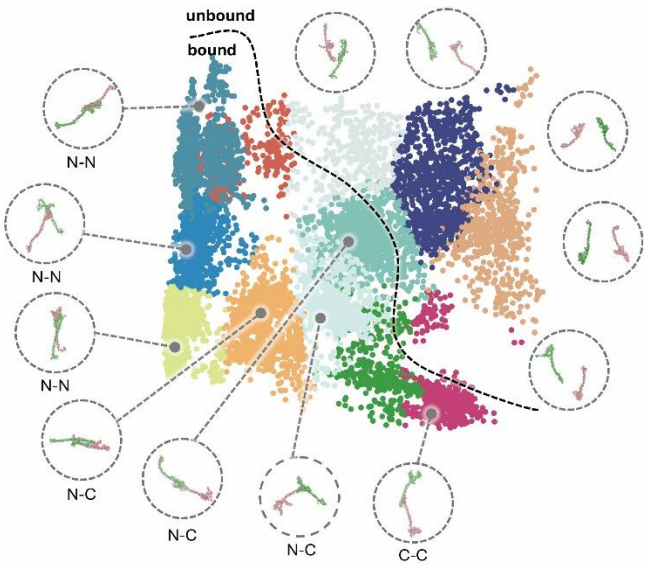

Supplementary Fig. 12. Principal components analysis (PCA) of CAHS12 dimer conformations from unbiased simulations. Each point represents a simulation frame projected onto the first two PCs derived from inter-protein features. Colors correspond to distinct binding modes identified via k-means clustering. The dashed line denotes the boundary between bound and unbound dimer states. Protein structures corresponding to representative binding modes were rendered using Visual Molecular Dynamics (VMD)[16].

In the Methods section, we also made the corresponding changes.

'… To investigate the interaction modes underlying CAHS12 protein assembly into networks, we performed nine independent unbiased simulations with each containing two CAHS12 proteins. The proteins were initially positioned in a 30 nm cubic water box with sufficient separation to prevent direct interactions. Each system underwent energy minimization, followed by 5 ps of constant volume and temperature (NVT) equilibration and 10 ns of NPT equilibration. A 1000 ns production run was then conducted for each replicate to allow for the formation of dimers. …'

8. Fig. 2D – Nothing wrong with this analysis, but this was already known Tanaka et al., and Sanchez-Martinez et al. though no prior credit is given to the authors of these papers for their contributions, rather this result is presented as novel.

Response: We thank the reviewer for this important comment. We note that the relevant studies by Tanaka *et al.* and Sanchez-Martinez *et al.* were cited earlier in the manuscript[1,5], but we agree that their contributions were not sufficiently discussed in the context of **Fig. 2D**. To address this, we have modified the text to more explicitly situate our results within the framework established by these prior experimental studies. To our knowledge, the results presented here represent the first molecular simulation data for CAHS12 that are directly consistent with these experimental observations. Such agreements also further lend confidence to our simulation protocol and interpretation. We have revised the main text accordingly and reproduced the changes below for convenience.

*'… These results highlight the critical role of the N-terminal region as a "sticky" end that promotes aggregation and filament formation, potentially serving as mechanical support for membrane architectures during dehydration, and providing a putative rationale for the experimentally observed role for the N-terminus in conferring protective function (**Fig. 1B, Supplementary Fig. 6**). These simulation results agree with prior experimental observations demonstrating that CAHS protein mutants can form diverse molecular assemblies and confer protective effects[1,5].'*

9. Fig. 2E – I think this experiment has a major flaw that is leading to incorrect conclusions. Here, only POPC (which is mostly on the outer leaflet) was used which is a neutral lipid so you would expect to only get hydrophobic residues interact. Why not test with anionic lipids which are on the inner leaflet and so more biologically relevant? The charged, amphipathic linker is more likely to interact with these anionic lipids. Simulating POPC alone is not biologically relevant and I fear this will give readers the wrong impression (that the termini interact with the membrane and the linker does not). Also – I would suggest that the authors examine the literature on LEA proteins (disordered proteins with similarities to CAHS proteins). Particularly looking at work from the Thalhammer lab on LEA protein/membrane interactions would be a good starting point for starting to understand what the field has already determined vis-à-vis desiccation-related IDP/membrane interactions. I think you will see that the linker is the much more likely site of interaction, but that the use of POPC is creating an artefact that shows the opposite.

Response: We thank the reviewer for this insightful and constructive comment. We fully agree that membrane composition plays an important role in modulating CAHS protein-membrane interactions, and that simulations employing neutral POPC bilayers constitute only part of the whole picture of how CAHS proteins interact with biological membranes. For example, Thalhammer group showed that the LEA protein, which shares important structural and functional similarities with CAHS proteins, presents a charged and amphiphilic helical structure and preferentially associates with anionic membrane surfaces, and that such interactions are critical to their protective function during dehydration and rehydration[17,18]. CAHS proteins have also been implicated in associating with lipid membranes[19]. These studies strongly support the view that linker domains also constitute key membrane-interacting motifs under physiologically relevant conditions.

As such, we extended our analysis to membranes containing increasing fractions of the anionic lipid POPG to approach this question. Our simulations reveal that incorporation of POPG substantially enhances the interaction of the charged linker region of CAHS12 with the membrane surface, while interactions with the termini persist (**Supplementary Fig. 19**). This trend is consistent with prior observations for LEA proteins and supports a mechanistic picture in which electrostatic interactions with anionic lipids play an important role in mediating linker-membrane association[17,18].

Nonetheless, we emphasize that the primary objective of this work is to provide molecular-level insights into how CAHS proteins stabilize synthetic POPC membrane systems relevant to minimal synthetic cells of interest for biotechnological and bioengineering applications, rather than

to fully recapitulate the complexity of native cellular membranes. Within this defined scope, our conclusions regarding CAHS-membrane interactions remain valid, but we agree that simulations employing only neutral lipids might give a misleading impression if interpreted without this context. Accordingly, we have revised the main text to cite relevant prior work and explicitly emphasize the sensitivity of CAHS-membrane interactions to lipid composition.

We thank the reviewer again for prompting these clarifications, which have strengthened both the interpretation and presentation of our results. We have made the changes to the section Molecular *dynamics simulations of CAHS12 protein assemblies reveal key interactions with POPC membranes* and reproduced the changes here for your convenience.

'… In addition to mediating protein-protein interactions, we hypothesized that the CAHS12 protein may also mediate protein-lipid interactions, anchoring or stabilizing membrane structures under desiccation. Such an idea has been speculated for tardigrade disordered proteins by Bino et al. and Hesgrove et al.[19,20]. …'

*'… Trajectory analysis revealed three distinct protein–membrane interaction modes, involving membrane association mediated by the N- and C-terminal regions and the proximity of the α-helix linker to the membrane (**Supplementary Fig. 18**), suggesting a variety of mechanisms by which CAHS12 engages with lipid structures. Prior studies have shown that the interaction patterns between CAHS12 proteins and phospholipid membranes are sensitive to membrane composition[17,18]. Increasing the fraction of the anionic lipid POPG in the membrane enhances the contact frequency of the linker region while preserving the high contact frequency of the terminal regions (**Supplementary Fig. 19**), indicating that the terminal domains, along with the linker domain, cooperate in the interaction with lipid membrane[10]. In this study, we focus on POPC membranes in that they offer a well-defined reference system for investigating the utility of CAHS12 in the context of synthetic cells with POPC membranes. As such, our simulation results are intended to characterize CAHS12 interactions with neutral POPC membranes and are not necessarily transferable to the understanding of CAHS12 interactions with natural biological membranes.'*

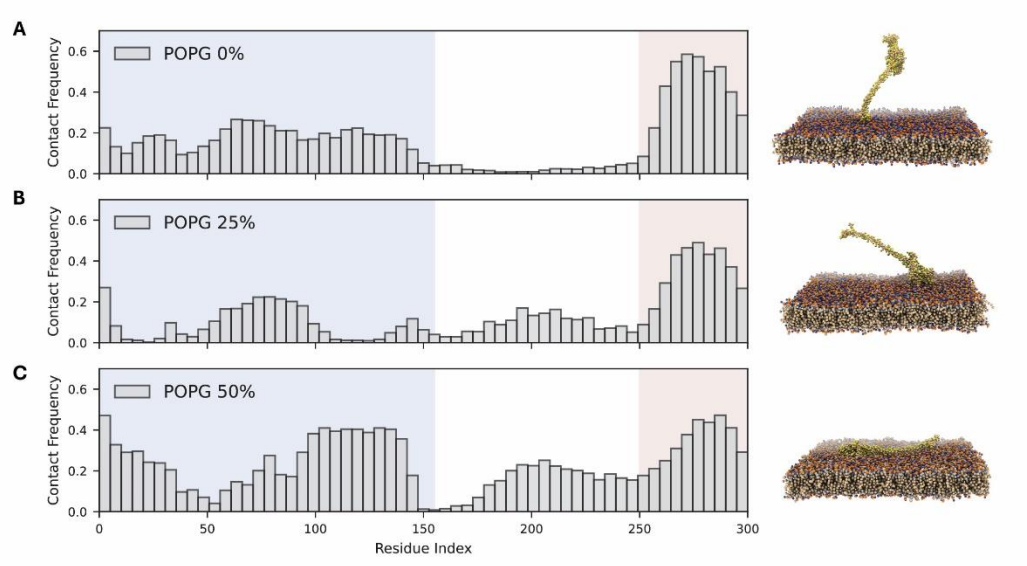

Supplementary Fig. 19*. Membrane composition modulates CAHS12-membrane interactions. The residue level contact frequency of CAHS12 with POPC bilayers containing 0% (A), 25% (B), and 50% (C) POPG, along with their representative snapshots of the corresponding simulations. An increasing percentage in the POPG composition corresponds to increasing membrane surface charge and an observed increase in interactions between the linker region and the membrane. A contact is defined when the minimum distance between any residue atom and a lipid phosphate bead is less than 1 nm, and the contact frequency is reported as the fraction of simulation time each residue spends in contact with the membrane. Data were obtained from three independent simulations totaling 5 μs for each membrane composition and concatenated for analysis. To reduce local fluctuations and highlight regional trends along the sequence, contact frequencies are averaged over sliding windows of five residues, with each bar representing the mean value within a window. The simulation snapshots were rendered using ChimeraX.*

10. Fig. 2F what are the percentages displayed here. No text in the figure legend specifying this.

Response: We thank the reviewer for the careful reading. The percentage shown in **Fig. 2F** corresponds to the fraction of remaining water beads relative to the initial simulation box, such that a lower percentage indicates that a larger amount of water has been removed. We have clarified this definition by explicitly adding it to the caption of **Fig. 2F**.

'Fig. 2. *(**F**) Residue-level membrane contact analysis for CAHS12, CAHS12 ΔC, and CAHS12 ΔN during progressive water removal simulations (i.e., increasing protein concentration), along with the molecular visualization showing the CAHS12 protein and POPC membrane, mimicking*

the desiccation process. The percentage indicates the fraction of remaining water beads relative to the initial simulation box, with a lower value corresponding to a greater extent of water removal. Contacts are defined as the number of unique residues that are within 0.5 nm of POPC lipid headgroups, normalized by the number of CAHS12 proteins.'

11. Fig. 3A – Why are different time points shown for CAHS12-GFP and CAHS12deltaN (e.g., 74 vs. 14 days)? Please show matching timepoints to aid in comparison. Also, why are only two of the four proteins used in this study shown here?

Response: We appreciate the reviewers' insightful comments. The original version of **Figure 3A** showed CAHS12-GFP (74 days) at different time points compared to CAHS12ΔN (14 days), as this was intended to more strongly demonstrate that the dehydration mechanism based on CAHS provides long-term protection for GUVs. Additional time points for CAHS12-GFP (14 days and 30 days) are presented in **Supplementary Fig. 21A**. As requested by the reviewers, matching time points (14 days for both proteins) have now been added for CAHS12-GFP, CAHS12, CAHS12ΔC, and CAHS12ΔN. The updated data are presented in the revised **Supplementary Fig. 21A**, enabling a clear comparison of stability among different constructs.

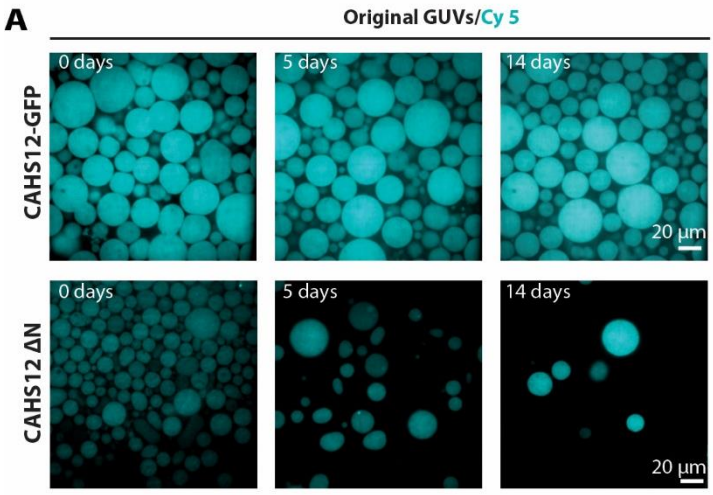

Fig. 3. CAHS12 enhances GUV stability during storage, dehydration, and osmotic stress. (**A**) Confocal images of GUVs containing Cy5 stored at room temperature. GUVs containing 280 µM CAHS12-GFP or CAHS12 ΔN were stored for 0–14 days.

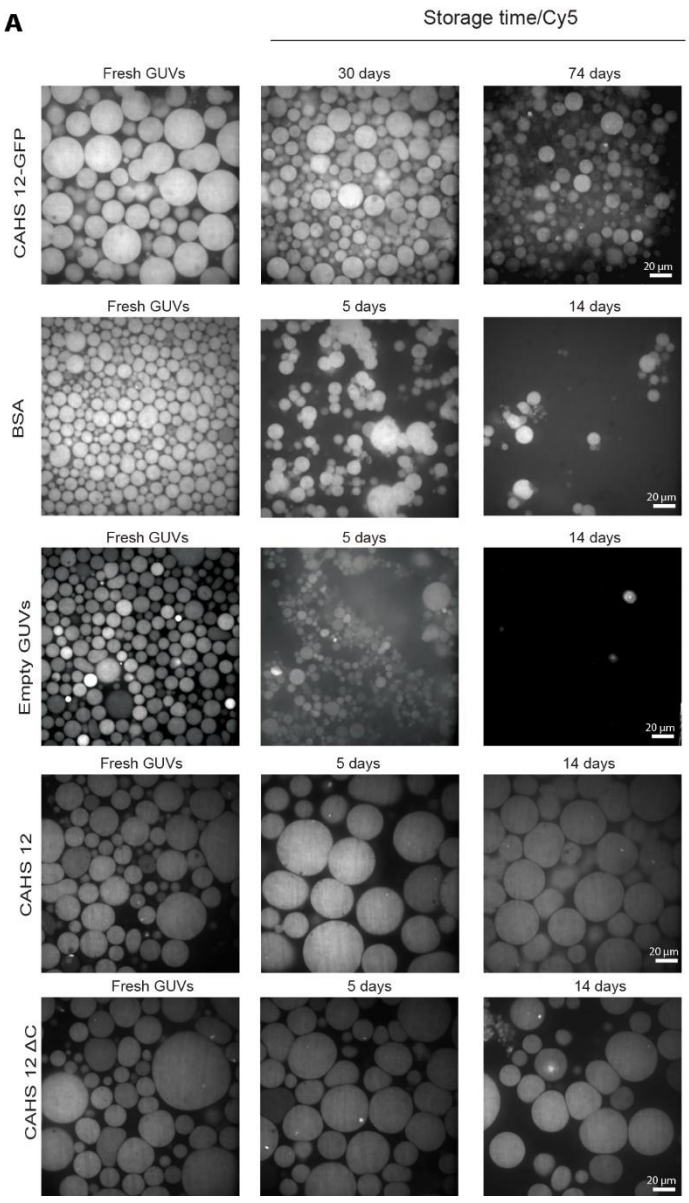

Supplementary Fig. 21. Long-term ambient storage stability of empty GUVs and GUVs encapsulating CAHS12-GFP, BSA, CAHS12, or CAHS12 ΔC. (**A**) Confocal fluorescence microscopy images of GUVs co-encapsulating Cy5 dye and either 280 μM CAHS12-GFP, BSA, CAHS12, or CAHS12 ΔC, imaged after storage under ambient conditions. Scale bar, 20 μm.

12. Fig. 3B CAHS12-GFP looks so much better than CASH12 alone. Where is the GFP only control?

Response: We thank the reviewer for the comment. Although CAHS12–GFP appears to better preserve GUV morphology in the representative images of **Fig. 3B**, our quantitative measurements show no significant difference in protective capability between CAHS12 and

CAHS12–GFP. The apparent visual difference mainly reflects sample-to-sample variation in GUV size, as GUVs encapsulating untagged CAHS12 tend to be smaller, which can make loss of integrity appear more pronounced.

We did perform a GFP-only control, which is the appropriate comparison for the CAHS12–GFP construct. GFP alone does not prevent GUV collapse or cargo leakage following dehydration/rehydration and behaves equivalently to BSA or CAHS12 ΔN-only conditions. These experiments were conducted under identical buffer, dehydration, and imaging conditions as all CAHS12 constructs. The GFP-only control has now been added to **Supplementary Fig. 3A**, and the figure legend has been updated to clarify this point.

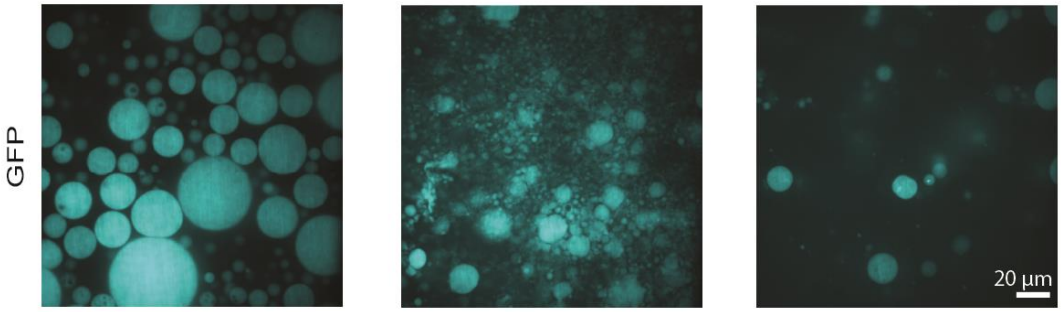

Supplementary Fig. 3. (**B**) Fluorescence microscopy images of GUVs encapsulating GFP under fresh (left), dehydrated (middle), and rehydrated (right) conditions. Cy5 dye was co-encapsulated as a membrane integrity reporter. Dye retention indicates vesicle stability, while loss of fluorescence reflects membrane rupture or leakage.

13. Fig. 3C – All four proteins tested here, which is great – but leads me to wonder why in A, C, D, E, and F only a subset of the proteins are used.

Response: We thank the reviewer for this observation. In **Fig. 1B**, we included all four proteins to provide a comprehensive comparison of their protective capability. As shown in Fig. 1, CAHS12, CAHS12–GFP, and CAHS12ΔC exhibit highly similar protection of GUVs, whereas CAHS12ΔN shows markedly reduced activity. Based on these established functional relationships, we used representative members from each functional class in panels A, C, D, E, and F.

This design allowed us to present the most relevant comparisons without repeating nearly identical traces across multiple figure panels. To ensure completeness, we have now added the time-stability and thermal-stability data for the remaining variants (CAHS12 and CAHS12ΔC) to **Supplementary Fig. 21A** and **Supplementary Fig. 22C**, respectively.

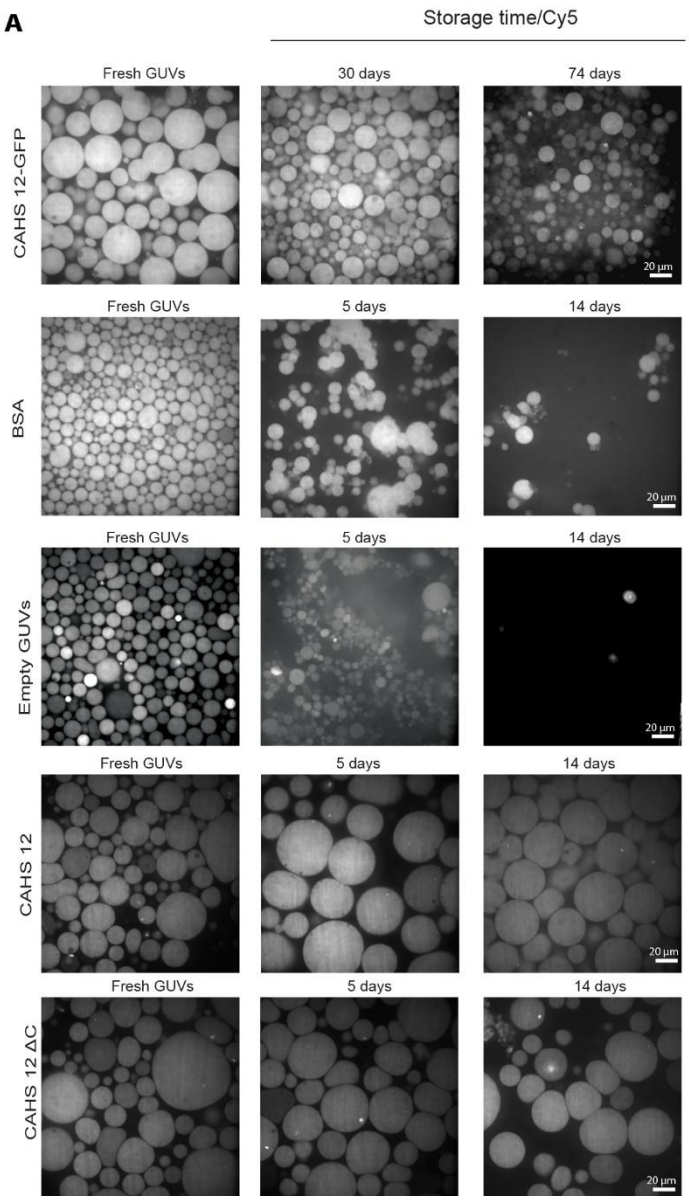

Supplementary Fig. 21. Long-term ambient storage stability of empty GUVs and GUVs encapsulating CAHS12-GFP, BSA, CAHS12, or CAHS12 ΔC. (**A**) Confocal fluorescence microscopy images of GUVs co-encapsulating Cy5 dye and either 280 µM CAHS12-GFP, BSA, CAHS12, or CAHS12 ΔC, imaged after storage under ambient conditions. Scale bar, 20 µm.

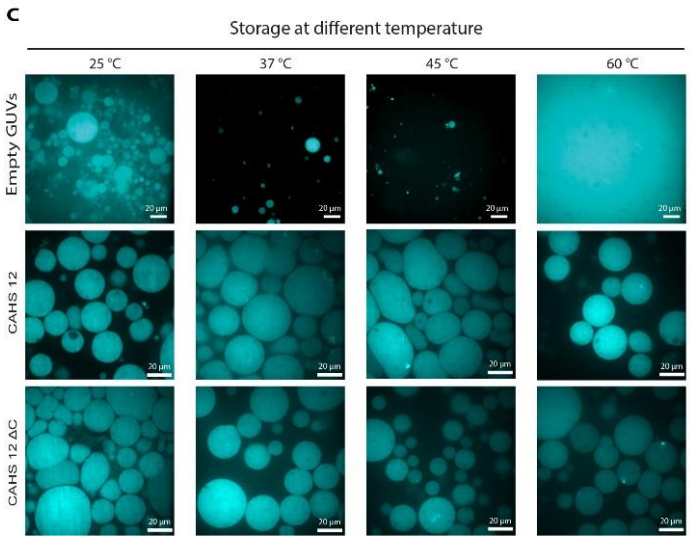

Supplementary Fig. 22. (**C**) Representative confocal fluorescence micrographs of empty GUVs, CAHS12 or CAHS12ΔC after incubation at 25 °C for 12 hours, 37 °C for 12 hours, 45 °C for 12 hours, and 60 °C for 2 hours. Elevated temperatures induced a marked reduction in vesicle size, consistent with heat-driven membrane remodeling or collapse. Scale bar, 20 µm.

14. Fig. 3D Why were different times used for each heating event (not reported for 80C)? Survival rate is not the best term to describe something that was never alive. Where is CAHS12-GFP and deltaC?

Response: We thank the reviewer for raising these questions. The 80 °C dataset was included in **Supplementary Fig. 22A** in the original submission. To avoid confusion, we have clarified this in the revised **Fig. 3D** legend and now explicitly reference the corresponding supplementary figure. We agree that “survival rate” is not appropriate for non-living vesicles. We have revised the figure and text to use the more accurate term “retention fraction”. The temperature-stability data for GUVs containing CAHS12 and CAHS12ΔC have now been added to **Supplementary Fig. 22C**.

As described in **Fig. 1B**, these variants show similar protective performance to CAHS12, and therefore only the representative protein was displayed in the main figure for clarity. The full dataset is now available in the supplementary materials.

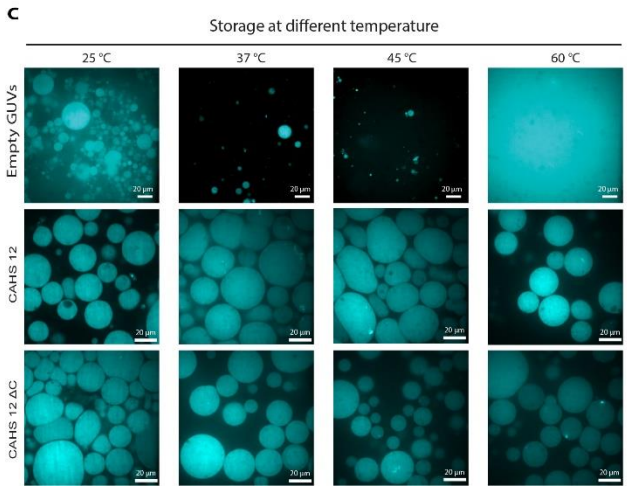

Supplementary Fig. 22. (**C**) Representative confocal fluorescence micrographs of empty GUVs, CAHS12, or CAHS12 ΔC after incubation at 25 °C for 12 hours, 37 °C for 12 hours, 45 °C for 12 hours, and 60 °C for 2 hours. Elevated temperatures induced a marked reduction in vesicle size, consistent with heat-driven membrane remodeling or collapse.

15. Fig. 4 – Broadly, Figure 4 demonstrates in a few different ways that CAHS proteins can protect other proteins/enzymes during drying. This is fine; however many prior studies have shown this and yet the results here are presented as novel. Please give credit to prior works that demonstrated this.

Response: We thank the reviewer for highlighting the substantial prior literature demonstrating that intrinsically disordered proteins, including CAHS proteins, can protect other proteins and enzymes during drying.

Several earlier studies have shown that purified CAHS proteins protect labile enzymes against desiccation-induced loss of activity in vitro. For example, CAHS proteins have been demonstrated to preserve the catalytic activities of lactate dehydrogenase (LDH) and lipoprotein lipase following desiccation, freezing, and lyophilization, supporting the potential use of CAHS proteins as stabilizing excipients for labile enzymes and biologics[1,8,10,12]. These findings were first reported by Piszkiewicz *et al.* in 2019 and are consistent across multiple follow-up studies in the field[8]. More recent work has further refined our understanding of how CAHS and related proteins confer protection during drying. For instance, a 2025 study in *Protein Science* demonstrated that the solution versus gelled phase of CAHS D differentially affects its protective capacity for different client enzymes, linking phase behavior to protective outcome[12].

Considering these contributions, we have revised the Discussion to clearly acknowledge these prior demonstrations of enzyme protection by CAHS proteins and to place our current results in this context. Specifically, we now reference the above reports as foundational work showing that CAHS proteins can stabilize enzymes during desiccation and then emphasize how Fig. 4 extends this knowledge by systematically comparing protection across multiple CAHS variants and using more stringent structural and mechanistic readouts.

Revised text for the Discussion

"Prior studies have established that CAHS proteins can act as protein stabilizers during drying, preserving enzymatic activity in vitro[1,8,10,12]*. Our results confirm and extend these findings by demonstrating that sequence-based variants of CAHS differ in their efficacy across client molecules and environmental conditions, suggesting mechanisms by which intrinsic disorder and phase behavior tune desiccation protection."*

16. Fig. 4B – mCherry signal already present at 0 hour and then there is still fluorescence after rehydration to me this implies that the signal was there before drying and that you preserved mCherry, not the ability to translate mCherry encoding RNA. A western showing mCherry levels going up after rehydration would show that translation is still happening.

Response: We thank the reviewer for this careful observation. **Figure 4B** shows fluorescence microscopy images of cell-free expression (CFE) in dehydrated GUVs after rehydration following storage at room temperature for varying durations (0 to 40 days). 0 day indicates GUVs that were dried and immediately rehydrated (i.e., stored for 0 days) to activate the CFE reaction, producing mCherry.

Other time points (e.g., 10, 20, 40 days) represent independent samples that were dried and stored for the indicated durations before rehydration and activation of the CFE reaction. Thus, the mCherry fluorescence observed at 0 day confirms that mCherry can be produced immediately upon rehydration, while each subsequent time point independently tests the preservation of the system over storage. These results demonstrate the maintenance of CFE activity in dehydrated GUVs over time, rather than reporting the translational capacity of mCherry-encoding RNA at 0 days.

17. Fig. 4B&J – missing control GUV without CAHS12. E.g., how do we know the transporter breaks when dried?

Response: We thank the reviewer for highlighting the importance of CAHS12-free GUV controls. Control experiments without CAHS12 for **Fig. 4B** are shown in **Supplementary Fig. 25B**, where GUVs fail to retain cargo after drying and rehydration, indicating loss of membrane integrity in the absence of CAHS12.

In **Supplementary Fig. S28**, we present a CAHS12-free control designed to assess whether membrane-anchored proteins remain functional after dehydration and rehydration in the absence of CAHS12. In this experiment, GUVs were decorated with a SpyTag-BFP fusion protein covalently attached to the membrane via a SpyCatcher lipid anchor. The SpyTag–SpyCatcher system serves solely as a stable membrane anchor and fluorescence marker to confirm the presence and continuity of membrane-associated proteins after dehydration–rehydration; it does not itself confer protection or transport activity.

Cy5 fluorescence in these images reports the presence of soluble cargo in the lumen of the GUVs. The diffuse Cy5 signal observed throughout the image field reflects cargo leakage into the external solution following dehydration and rehydration, indicating loss of membrane integrity in the absence of CAHS12. The patchy or blotchy appearance of the SpyTag-BFP signal after rehydration reflects partial membrane disruption and heterogeneous retention of membrane-anchored proteins, a phenomenon commonly observed following severe dehydration stress. Importantly, this nonuniform distribution contrasts with the continuous membrane localization observed in CAHS12-containing GUVs and is consistent with the failure of the membrane-associated system in the absence of CAHS12.

We have revised the figure legend and corresponding text to explicitly clarify the roles of SpyTag-BFP and Cy5 in this experiment and to guide interpretation of the control data.

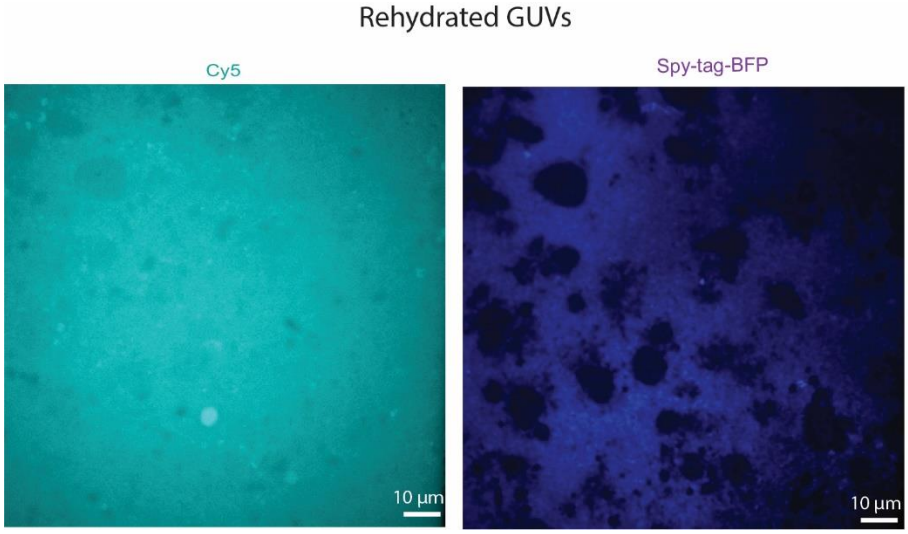

Supplementary Fig. 28. CAHS12-free control for GUV stability after dehydration–rehydration. Fluorescence microscopy images of GUVs lacking CAHS12 after dehydration and rehydration. GUV membranes are decorated with a SpyTag-BFP fusion protein covalently attached via a SpyCatcher lipid anchor, serving as a fluorescent marker for membrane-associated proteins (blue). Cy5 fluorescence reports soluble cargo. Following dehydration–rehydration, Cy5 signal is observed throughout the field, indicating cargo leakage from GUVs, while the SpyTag-BFP signal appears patchy and discontinuous, consistent with membrane disruption in the absence of CAHS12.

18. Fig. 4J – the merge panels are very pixilated please check resolution.

Response: We thank the reviewer for noting this issue. The pixelation in the merged panels of **Fig. 4J** resulted from the image export settings used in the initial submission. We have reprocessed the images and adjusted the resolution accordingly, and the revised figure now displays the merged panels at the appropriate resolution.

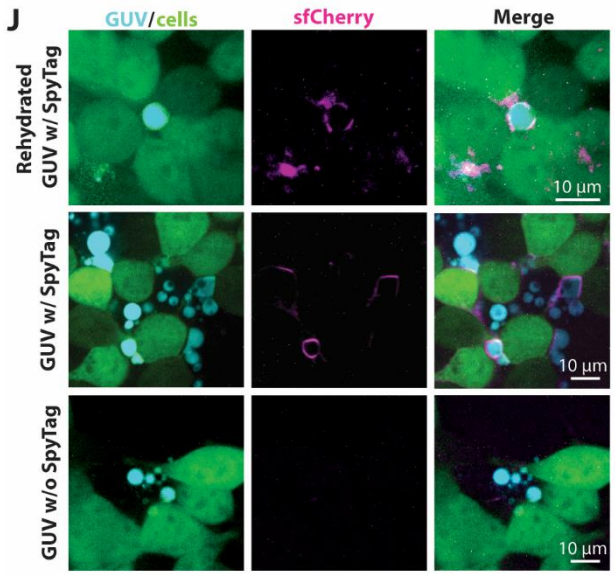

Figure 4. (J) Following incubation, sfCherry reconstitution between GUV and cells is observed with both freshly prepared and dehydrated/rehydrated SpyTag-BFP GUVs. No reconstitution is seen with GUVs lacking SpyTag-BFP.

19. Fig S2 – there are so many degradation bands on this gel. Are the authors purifying these degradation products and using them in their experiments? Also deltaN shows higher order oligomers which contradicts the simulations performed by the authors that suggest fewer interactions between this variant – please explain why there is a discrepancy here.

Response: We thank the reviewer for carefully examining **Supplementary Fig. 2** and for raising these important points. Regarding the multiple lower-molecular-weight bands, we agree that these likely reflect the presence of minor truncation or degradation products that arise during expression and purification, rather than stable species intentionally purified or used in downstream experiments. Importantly, we did not isolate or enrich any of these lower-molecular-weight bands, nor were they used independently in any functional assays. All experiments were performed using the bulk purified protein preparation.

We note that in the original gel, the relative prominence of these minor species was exacerbated by high protein loading. When the experiment was repeated using standard SDS–PAGE loading amounts, the dominant full-length band became clearly resolved, and the minor species were no longer prominent. We have therefore replaced the original gel with the updated SDS–PAGE data obtained under these conditions in the revised **Supplementary Fig. 2**.

With respect to the apparent higher-molecular-weight bands observed for the ΔN variant, we emphasize that SDS–PAGE is a strongly denaturing assay that can nevertheless preserve residual associations for intrinsically disordered proteins, particularly those enriched in charged or low-complexity regions. The faint higher-order bands observed under high-loading conditions do not indicate stable oligomerization in solution. Consistent with this interpretation, under adjusted loading conditions, the ΔN variant does not exhibit pronounced higher-order species.

Importantly, our molecular simulations address intermolecular interactions under dilute, non-denaturing conditions and predict reduced interaction propensity for the ΔN variant relative to full-length CAHS12. The revised biochemical data are fully consistent with this prediction, and the apparent discrepancy in the original figure arose from gel-loading and visualization conditions rather than from genuine contradiction between experiment and simulation.

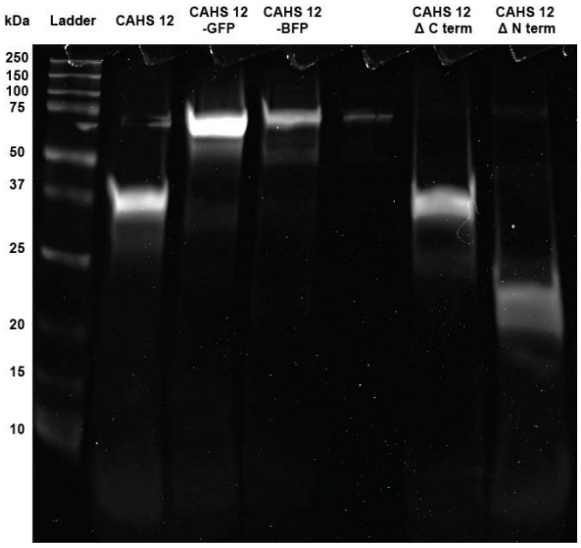

Supplementary Fig. 2. SDS–PAGE analysis of purified CAHS12 and truncation variants. Coomassie-stained SDS–polyacrylamide gel showing full-length CAHS12 and domain-deletion variants after Ni-NTA affinity purification. Lanes: molecular weight marker (kDa); 1, CAHS12; 2, CAHS12-GFP; 3, CAHS12-BFP; 4, CAHS12 ΔC; 5, CAHS12 ΔN. All proteins were expressed in *E. coli* BL21(DE3) and purified via His_6-tag affinity chromatography followed by buffer exchange into Tris-based storage buffer (pH 8.0). Predicted molecular weights: CAHS12, ~32 kDa; CAHS12-GFP, ~60 kDa; CAHS12-BFP, ~60 kDa; ΔC, ~29 kDa; and ΔN, ~16 kDa.

20. Fig. S5 – why was BFP used here instead of GFP which is used throughout the rest of the manuscript. I could not find a rationale/justification.

Response: We thank the reviewer for this question. BFP was used in **Supplementary Fig. 5** to confirm that the protective effect of CAHS12 on GUVs is independent of the fluorescent tag. Using a spectrally distinct fluorophore allowed us to demonstrate that replacing GFP with BFP does not affect CAHS12-mediated protection during dehydration and rehydration. This rationale has now been explicitly clarified in **Supplementary Table S7**.

Supplementary Table S7. *Assignment of CAHS12 constructs to experimental assays*

CAHS12 construct	***Tag***	***Primary purpose***	***Assays used***
CAHS12 (full length)	*None*	*Functional protection without tag interference*	*Long-term dry storage assays; interfacial tension measurements; thermal stability*
CAHS12–GFP	*GFP*	*Visualization of protein localization and assembly*	*Confocal imaging of GUVs; dehydration–rehydration dynamics; network formation; interfacial tension measurements; thermal stability*

CAHS12–BFP	*BFP*	*Visualization of protein localization and assembly*	*Confocal imaging of GUVs; Control to test tag effects on GUV protection*
CAHS12 ΔN	*None*	*Dissection of role of N-terminal region*	*GUV protection assays; interfacial tension measurements; stability comparisons*
CAHS12 ΔC	*None*	*Dissection of role of C-terminal region*	*GUV protection assays; interfacial tension measurements; stability comparisons*

21. Fig. S6 – Why were different concentrations used for different variants? Please justify.

Response: We thank the reviewer for pointing this out. Upon careful re-examination, we found that the concentration of CAHS12 ΔN was incorrectly labeled as 70 μM and should instead be 75 μM. This labeling error has now been corrected in the revised manuscript. Importantly, the experiments were performed using the correct concentration, and this correction does not affect the results or the conclusions drawn from **Supplementary Fig. 6**. We apologize for the confusion caused by this error and appreciate the reviewer's careful reading.

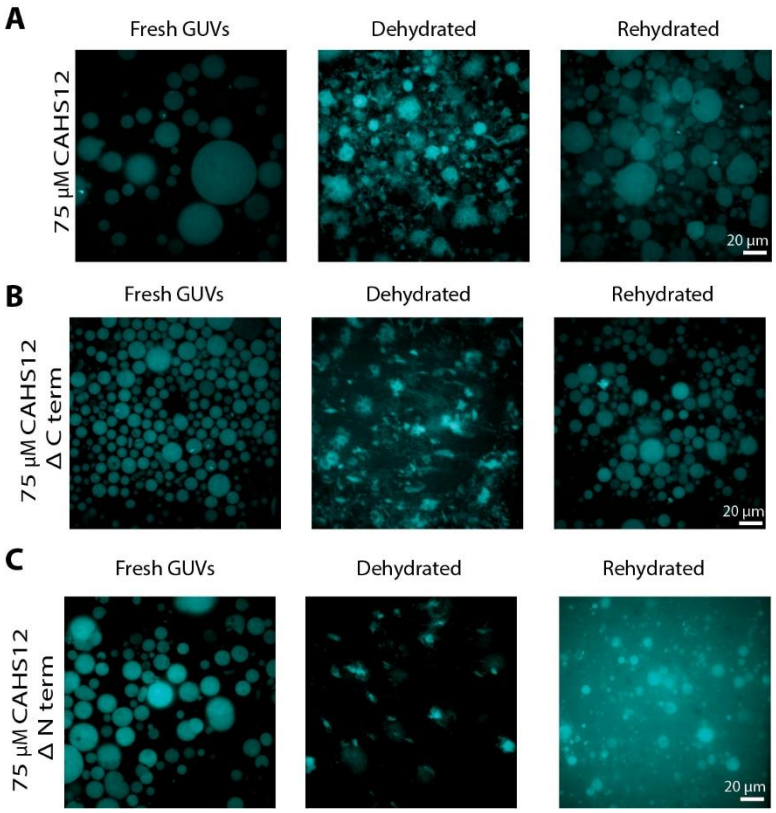

Supplementary Fig. 6. Functional contributions of CAHS12 termini to desiccation protection in GUVs. Fluorescence microscopy images of GUVs encapsulating 75 μM full-length CAHS12 (**A**), 75 μM C-terminal truncation (**B**), or 75 μM N-terminal truncation (**C**) under fresh, dehydrated, and rehydrated conditions. Cy5 dye was co-encapsulated as a membrane integrity

reporter. Full-length CAHS12 and ΔC maintained vesicle integrity following dehydration and rehydration, while ΔN failed to prevent membrane collapse or dye leakage. Representative images from ⩾3 independent experiments.

22. Fig. S8 Why were no statistics performed here to determine significance? Is the concentration dependence significant?

Response: We thank the reviewer for raising this point. In **Supplementary Fig. 8**, interfacial tension (IFT) measurements were performed using a hanging drop tensiometer, with three independent measurements per condition, and the data are presented as mean ± s.d. as stated in the figure legend.

The primary purpose of **Supplementary Fig. 8** was to demonstrate that CAHS12 modulates interfacial tension in a construct- and concentration-dependent manner, rather than to establish a statistically powered dose–response relationship. Given the limited number of independent measurements per condition (n = 3), we did not perform formal statistical significance testing between individual concentrations, as such analyses would not be sufficiently powered and could be misleading.

Nevertheless, the observed monotonic trends across the concentration range (0–1 mM), together with consistent differences between full-length CAHS12 and the ΔN truncation, support a clear qualitative concentration dependence. We have clarified this intent in the legend to emphasize that **Supplementary Fig. 8** is meant to illustrate concentration-dependent trends rather than statistically significant differences between specific concentrations.

23. Fig. S9 – Can the authors comment on why in the fresh GUVs are there so few and large in deltaN?

Response: We thank the reviewer for this insightful observation. While we do not have direct experimental evidence to definitively determine the origin of this size distribution, we agree that the effect is most plausibly attributed to events occurring during the GUV formation process rather than at the level of mature lipid bilayers. Specifically, in fresh preparations containing CAHS12 ΔN, the appearance of fewer but larger GUVs likely reflects altered stabilization of the water-in-oil droplets or intermediate emulsion structures from which GUVs are formed. The N-terminal region of CAHS12 may contribute to interfacial or membrane-proximal interactions that help regulate droplet size and prevent droplet fusion during GUV generation. Deletion of this region (ΔN) could reduce such stabilizing interactions, leading to the formation of larger precursor droplets and consequently fewer, larger GUVs after membrane closure. This interpretation is

consistent with the reduced protective activity of CAHS12 ΔN observed in dehydration and rehydration assays, suggesting that the N-terminal region contributes to interfacial or membrane-associated functions that influence both vesicle formation and subsequent stabilization under stress.

24. Fig. S10 – All this has previously been reported, but it is reported here as novel.
Response: We thank the reviewer for this important clarification and agree that the observations shown in **Supplementary Fig. 10** (The revised figure is now **Supplementary Fig. 11**) are consistent with previously reported results. Our intention in including **Supplementary Fig. 10** (now **Supplementary Fig. 11**) was to provide supporting evidence that our coarse-grained simulation protocol reproduces known experimental trends and thus validate the applicability of our computational approach in the context examined here. It was not our intent to present these data as novel findings. To clarify this intent, we have provided additional references when we first mention this figure, and the corresponding changes are shown below.

*'These secondary structure assignations result in a molecular model of a single CAHS12 protein in water possessing a radius of gyration (R_g) of (5.21 ± 0.11) nm, which falls in a similar regime for other tardigrade disordered proteins from prior studies (**Supplementary Fig. 11**)[1,5,7,21,22].'*

25. Fig. S19 – Prior work has shown that CAHS protein assemblages melt at around 40C. How do the authors imagine protection is taking place at 80C when CAHS assemblages would have been disrupted?
Response: We thank the reviewer for this insightful comment. Prior biophysical studies on CAHS proteins have shown that gel/assembly states of tardigrade CAHS proteins undergo thermal transitions at temperatures near ~40 °C when analyzed in vitro. Specifically, differential scanning calorimetry (DSC) and rheological measurements of CAHS D gels reveal a melting/gel–sol transition with a midpoint around ~308–310 K (~35–37 °C), consistent with reversible structural rearrangements in this temperature range under aqueous conditions[13].

However, the ability of CAHS proteins to confer protection at higher temperatures such as 80 °C does not necessarily require maintenance of large-scale gel assemblies at those temperatures. While gel-like supramolecular assemblies may be disrupted above their melting transitions, residual protein–membrane interactions, hydration effects, and local crowding can still provide stabilization of lipid membranes and encapsulated components at an elevated temperature. The intact gel structure per se is not a prerequisite for high-temperature protection,

and that thermal melting behavior measured in vitro may differ from behavior within the complex environment of dehydrated synthetic cells or GUVs.

26. Fig. S20 – It seems from the data that CAHS12-GFP causes GUVs to be very big – this in and of itself is a perturbation. If a cell doubles in size that's not necessarily a good thing. However, this was not observed in live cells in previous works (see Tanaka et al and Sanchez-Martinez et al). Do you think this difference might be an artefact of the GUV system? What species is this CAHS12 form?

Response: We thank the reviewer for this thoughtful comment. We agree that the apparent increase in GUV size observed in the presence of CAHS12-GFP represents a measurable perturbation of the synthetic system. Importantly, however, we believe this effect reflects system-specific properties of the GUV model rather than a contradiction of observations in living cells.

GUVs are minimal, cell-free systems that lack cytoskeletal structures, membrane trafficking, volume regulation, and active homeostatic mechanisms present in cells. As a result, protein–membrane or protein–interface interactions can manifest more directly during vesicle formation, leading to changes in vesicle size distribution that would be buffered or compensated in vivo. In contrast, live-cell studies, including those by Tanaka *et al.*[1] and Sánchez-Martínez *et al.*[5], examined CAHS protein behavior in the context of intact cellular machinery, where cell size is tightly regulated and not solely determined by passive mechanical or interfacial effects.

We therefore interpret the increased GUV size in the presence of CAHS12-GFP as a formation-stage or interfacial effect specific to the GUV system, rather than an indication of uncontrolled swelling or deleterious growth analogous to pathological cell enlargement. Notably, despite this size increase, CAHS12-containing GUVs remain structurally intact and display enhanced resistance to dehydration and rehydration stresses, indicating that the observed size change does not compromise vesicle integrity or function within this model system.

The CAHS12 construct used in this study is derived from *R. varieornatus*, a tardigrade known for desiccation tolerance. All constructs, including CAHS12-GFP, ΔN, and ΔC, are based on this species.

27. Fig. S1 "Desiccation" spelled "Dessication"

Response: The word "Dessication" in **Supplementary Fig. 1** has been corrected to "Desiccation" in the revised figure.

28. Fig. 1D seems out of place, why is this one panel out of four specifically labeled with “D”? Also C and D in the figure legend seem like they have been mixed up.

Response: We thank the reviewer for pointing out the potential confusion regarding panels C and D. To clarify:

- **Fig. 1C** shows a 3D fluorescence microscopy image of a Z-axis scan of dehydrated GUVs, highlighting the spatial distribution of CAHS12-GFP and the membrane dye.
- **Fig. 1D** shows a scanning electron microscopy (SEM) image of dehydrated GUVs, providing complementary structural information at higher resolution.

In the revised figure, the panel labels have been corrected and the legend updated as follows:

Z-axis scan 3D fluorescence microscopy image (C) and scanning electron microscopy image (D) of dehydrated GUVs. Magenta indicates membrane-localized Rhod-PE, while CAHS12-GFP is shown in gray (right and bottom left).

This clarifies the imaging modality for each panel and ensures consistency between the figure and legend.

Reviewer #2 (Remarks to the Author)

The manuscript “Cytoplasmic Abundant Heat-Soluble Proteins from Tardigrades Protect Synthetic Cells Under Stress” by Xi et al. describes a combination of experimental (scanning electron and optical microscopy, interfacial tension measurements) and computational (coarse-grained molecular dynamics simulations) studies of cytoplasmic abundant heat-soluble protein CAHS12, which, among other intrinsically disordered proteins, has been involved in protecting tardigrades from extreme environmental conditions (namely dessication, also elevated temperature, osmotic stress). The importance of this topic far exceeds the understanding of the physiology of these invertebrates, since it may open up exciting technological developments. The manuscript is well organized and clear. The experiments and simulations are well-designed and combine consistently to provide a picture that, under dessication, CAHS12 undergoes a reversible structural transformation (oligomerizes in a filamentous network, within the lumen of cell membrane-mimicking vesicles) that reinforces membrane integrity and protection, thus providing important new insights. I have the following minor comments:

Response: We thank the Reviewer for the positive and detailed evaluation of our manuscript. We are glad that the reviewer finds the study well organized and the combination of experimental and

computational approaches informative. We appreciate the recognition of the potential broader significance of CAHS12-mediated protection, and we are grateful for the constructive minor comments provided, which have helped us further clarify and improve the manuscript. Below, we provide point-by-point responses to each of the reviewer's minor comments.

1. Page 5 in the pdf file (no page numbers are actually provided): "Over the concentration range of 0.1–1.0 mM, CAHS12 exhibited a modest increase in interfacial tension (from ~12 to ~15 mN/m) (…) In contrast, the ΔN variant showed a more pronounced increase in IFT over the same range (from ~6 to ~8 mN/m)". As the numbers (and indeed the plots in Fig. 1I) show, the absolute IFT increase for the ΔN variant is not more pronounced than that for CAHS12.

Response: We thank the reviewer for this observation. We agree that the absolute increase in interfacial tension (Δγ) is numerically larger for CAHS12 (~3 mN/m) than for the ΔN variant (~2 mN/m). However, our original phrasing was referring to the relative increase with respect to the baseline interfacial tension. Specifically, ΔN shows a ~33% increase (from ~6 to ~8 mN/m), compared to ~25% for CAHS12 (from ~12 to ~15 mN/m). More importantly, the slope of γ vs. ln c is steeper for ΔN in this range, leading to a larger estimated surface excess (Γ), as determined via the Gibbs adsorption equation. To avoid this ambiguity, we have revised the sentence as follows:

"Although the ΔN variant exhibited a smaller absolute increase in interfacial tension (from ~6 to ~8 mN/m), the steeper slope in γ vs. ln c yielded a larger estimated surface excess (Γ ≈ 1.4×10⁻⁶ mol/m²), suggesting more extensive interfacial accumulation."

2. Page 21: "upper and lower boundaries of the lipid headgroup region" – these boundaries may have been defined from the z positions of adequate CG beads, please explain in more detail.

Response: We thank the reviewer for the clarification of determination of the boundaries of lipid headgroup region. We have revised the Methods section to include details of this implementation.

'A residue was classified as membrane-inserted if its Z-position fell within the vertical extent defined by the upper and lower boundaries of the lipid headgroup region. For each residue in the protein, the residue center of mass (COM) was projected onto the membrane plane, and all POPC NC3 headgroups within 8 Å of the COM position in the XY plane were selected. The Z-coordinates of these headgroups were then used to define a local membrane profile. The median of these Z-

coordinates was used to separate the headgroups into upper and lower leaflet populations. The mean leaflet Z-positions were computed for both leaflets, and the membrane midplane was defined as the average of the upper and lower leaflet means. A residue was considered inserted if its COM Z-position lay between the midplane and the mean position of the nearest leaflet. This criterion ensured that only residues embedded within the membrane interface, rather than merely in proximity to it, were counted as forming meaningful membrane contacts.'

3. Page 31, legend of Fig. 1A: "CAHS12 disassembles from the membrane interface, releasing tension and allowing fluidity of lipids on the membrane (…)" – actually the part about membrane order/fluidity has not been validated from this study, although the MD simulations could provide an adequate test, which the authors should consider doing.

Response: We thank the reviewer for this comment and agree that membrane fluidity was not directly measured in this study. The images shown here illustrate morphological and mechanical responses of GUVs under micropipette aspiration, rather than direct changes in lipid order.

As shown in **Supplementary Fig. 9**, GUVs containing full-length CAHS-12 or the CAHS-12 ΔC variant resist elongation under an aspiration pressure of 2660 Pa, in contrast to the ΔN variant, which deforms more readily. Quantitative analysis of tension versus areal strain relationships obtained from micropipette aspiration measurements reveals corresponding differences in the apparent area expansion modulus. Specifically, GUVs containing CAHS-12 ΔC exhibit a higher apparent area expansion modulus (76.9 ± 15.8 mN/m), followed by full-length CAHS-12 (61.3 ± 10.0 mN/m), whereas the ΔN variant displays a substantially lower modulus (21.6 ± 1.3 mN/m), indicating reduced mechanical resistance to membrane deformation.

Consistent with these results, increasing concentrations of CAHS-12–GFP progressively increase the apparent area expansion modulus, from 39.9 ± 6.1 mN/m at 0.05 mM to 51.5 ± 9.7 mN/m at 0.3 mM and 67.6 ± 9.0 mN/m at 0.9 mM, reflecting enhanced resistance to aspiration-induced strain. Across all conditions, tension–strain relationships were well described by linear fits (R-squared approximately 0.85 to 0.99.

These data demonstrate that CAHS-12 modulates membrane mechanical stability in a concentration- and domain-dependent manner, enhancing resistance to deformation rather than directly establishing changes in membrane fluidity. We have therefore revised the figure legend and associated text to remove explicit claims regarding lipid fluidity and instead frame the results in terms of mechanical stabilization, which is directly supported by the micropipette aspiration measurements presented in **Supplementary Fig. 9**. Additional methodological details describing the micropipette aspiration analysis have been added below.

Results and Discussion

*….. Consistent with these interfacial measurements, we performed micropipette aspiration experiments of CAHS12-containing GUVs to further demonstrate construct- and concentration-dependent mechanical stabilization of GUVs by CAHS12 (**Supplementary Fig. 9**) ……*

Micropipette aspiration.

Micropipettes were pulled from standard borosilicate glass capillaries (World Precision Instruments) using a P-87 pipette puller (Sutter Instruments) and fire-polished with a microforge (MF-83, Narishige) to yield an inner diameter of 8–10 µm. Micropipettes were mounted in a holder and connected via a continuous fluidic line to a filling syringe and a pressure reservoir through a three-way valve. The reservoir was pneumatically coupled to a high-speed pressure clamp (HSPC, ALA Scientific Instruments), allowing precise control of aspiration pressure.

The filling syringe contained a glucose solution osmotically matched to the external solution of the GUVs and was used to fill both the micropipette and the reservoir. All air bubbles were carefully eliminated from the system, as their presence compromises pressure stability during aspiration measurements. Using a micromanipulator, the micropipette was positioned in close proximity to a target GUV. Once the GUV was aligned, controlled negative pressure was applied via the pressure transducer to induce membrane aspiration into the micropipette. The applied suction pressure ΔP generates a uniform membrane tension τ in the vesicle membrane. The membrane tension is determined by the geometry of the system and depends on the inner radius of the micropipette (R_p) and the instantaneous radius of the vesicle exterior to the micropipette (R_{GUV}), according to:

$$\tau = \frac{(R_p \Delta P)}{\left(2\left(1 - \frac{R_p}{R_{GUV}}\right)\right)}$$

The apparent membrane area strain (ΔA/A) was calculated from the aspirated tongue length L, the pipette radius (R_p), and the vesicle geometry. The change in membrane area was normalized by the initial vesicle surface area, defined by the unstressed vesicle radius ($R_{0,GUV}$), yielding:

$$\frac{\Delta A}{A} = \frac{\left(2\pi\, R_p \Delta L \left(1 - \frac{R_p}{R_{GUV}}\right)\right)}{\left(4\pi\, R_{0,GUV}^2\right)}$$

To determine the membrane area stretch modulus (K_a), the membrane tension τ was plotted as a function of the direct area expansion ($\Delta A/A$). The resulting linear relationship was fit by least-squares regression, and the slope of this plot corresponds to the area stretch modulus K_a[23,24].

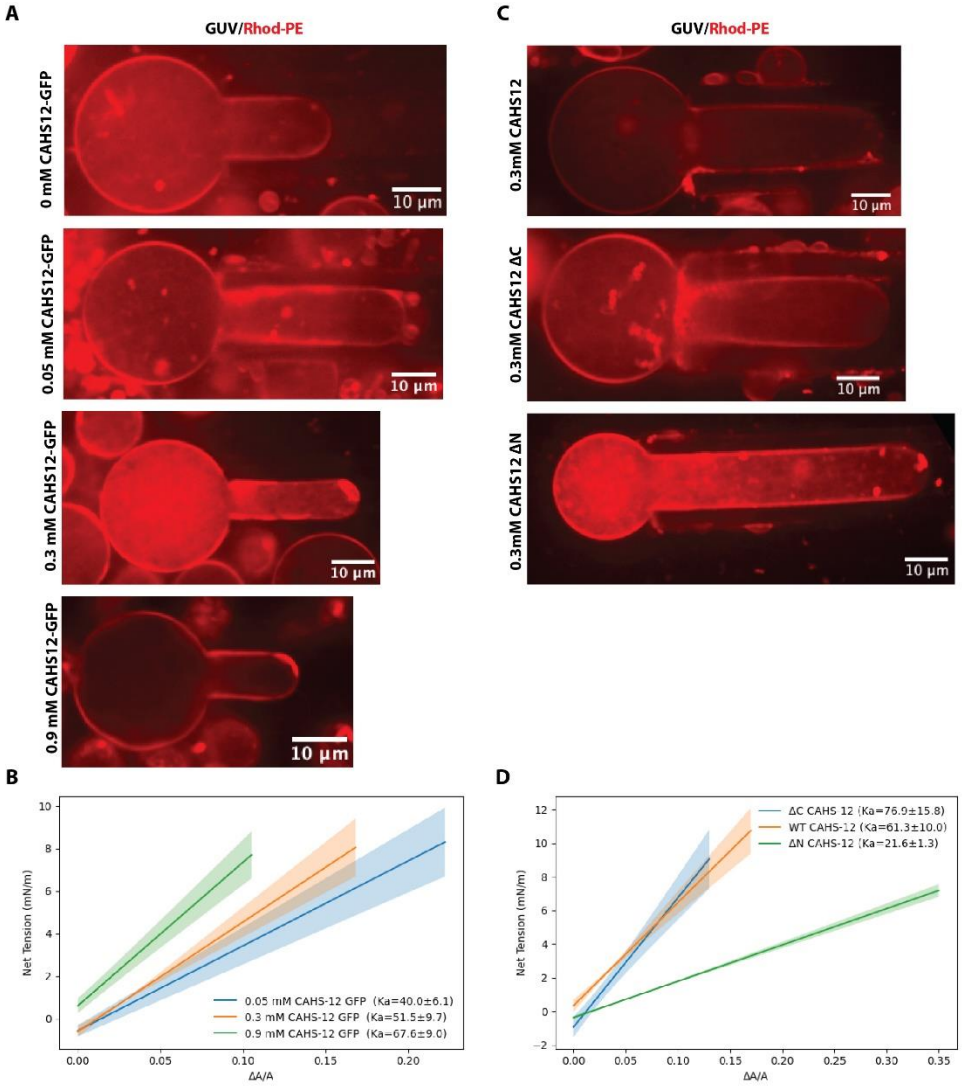

Supplementary Fig. 9. Micropipette aspiration reveals construct- and concentration-dependent mechanical stabilization of GUVs by CAHS12. Representative fluorescence microscopy images of Rhod-PE–labeled GUVs (red) subjected to micropipette aspiration at an applied aspiration pressure of 2660 Pa. (**A**) GUVs encapsulating increasing concentrations of CAHS12–GFP (0, 0.05, 0.3, and 0.9 mM) show a concentration-dependent increase in resistance to deformation under applied membrane tension. Empty GUVs exhibit relatively short aspiration lengths, likely due to higher initial membrane tension limiting available excess area. At low CAHS12 concentration (0.05 mM), partial membrane adsorption transiently increases effective deformability, whereas at higher concentrations (≥0.3 mM), interfacial protein networks

mechanically stabilize the membrane, reducing aspiration length. **(B)** Concentration-dependent modulation of membrane mechanics by CAHS-12–GFP. Linear fits to net membrane tension versus areal strain are shown for GUVs containing increasing concentrations of CAHS-12–GFP (0.05, 0.3, and 0.9 mM). Solid lines represent the mean linear fit across three independent replicates for each concentration, with shaded regions indicating plus or minus one standard deviation across replicate fits. The apparent area expansion modulus (K_a) increases with CAHS-12–GFP concentration, from 40.0 ± 6.1 mN/m at 0.05 mM to 51.5 ± 9.7 mN/m at 0.3 mM and 67.6 ± 9.0 mN/m at 0.9 mM, indicating enhanced resistance to aspiration-induced deformation. Linear fits for individual replicates yielded R-squared values ranging from 0.84 to 0.98 (0.05 mM), 0.91 to 0.97 (0.3 mM), and 0.94 to 0.99 (0.9 mM). N = 3 independent experiments. (**C**) GUVs encapsulating full-length CAHS12, CAHS12 ΔC, or CAHS12 ΔN at the same protein concentration. GUVs containing full-length CAHS12 or CAHS12 ΔC largely retain a spherical morphology during aspiration, whereas GUVs containing CAHS12 ΔN exhibit pronounced elongation, indicating reduced mechanical stability. **(D)** Quantification of K_a from linear fits to net membrane tension versus areal strain obtained by micropipette aspiration of GUVs containing CAHS-12 variants. Solid lines represent the mean linear fit across three independent replicates for each condition, with shaded regions indicating plus or minus one standard deviation across replicate fits. GUVs containing the C-terminal deletion mutant (ΔC CAHS-12) exhibit the highest apparent Ka (76.9 ± 15.8 mN/m), followed by wild-type CAHS-12 (61.3 ± 10.0 mN/m), whereas the N-terminal deletion mutant (ΔN CAHS-12) shows a substantially reduced modulus (21.6 ± 1.3 mN/m). Linear fits for individual replicates showed strong agreement, with R-squared values ranging from 0.85 to 0.97 (ΔC), 0.96 to 0.99 (WT), and 0.82 to 0.96 (ΔN).

4. The authors have provided simulation setups, scripts, and analyses related to this study. Although no trajectories are made available, the provided files constitute useful resources for someone willing to take inspiration for new work.

Response: We appreciate this comment by the reviewer. We have updated the repository to include the full set of input files from the additional simulations performed during the revision, along with corresponding analysis scripts where applicable. While full trajectories are not provided due to their size, the shared materials document the simulation setups and workflows, and we expect them to be useful resources for readers seeking to reproduce or build upon this work.

Reviewer #3 (Remarks to the Author):

This manuscript by Xi et al. not only confirms the protective role of CAHS12 on GUV phospholipid membranes during dehydration-rehydration cycles but also precisely identifies its N-terminal disordered region as the critical functional domain. Furthermore, it successfully demonstrates the ability to preserve the functionality of both cell-free transcription-translation (CFE) systems encapsulated within GUVs and membrane proteins incorporated into the phospholipid bilayer under long-term dry storage. This manuscript provides an interesting method to maintain the artificial cell stability. I would like to recommend it for publication after addressing below points.

Response: We thank Reviewer #3 for the positive review and for recognizing the impact of this work on enhancing artificial cell stability.

1. Figure 1G shows the redistribution of CAHS12-GFP during the rehydration process. Would it be possible to monitor the distribution changes of CAHS12-GFP a during the dehydration and rehydration process? How many cycles do those artificial cells undergo dehydration-rehydration?

Response: We thank the reviewer for this thoughtful question. In **Fig. 1G**, we focused on monitoring the redistribution of CAHS12–GFP during the rehydration process, as this step allows reliable real-time fluorescence imaging under well-controlled optical conditions.

In contrast, directly imaging protein redistribution during dehydration is technically challenging primarily because it is difficult to impose a controlled and reproducible drying condition under the microscope. While changes in refractive index accompanying solute concentration increase have only a minor effect on fluorescence imaging, the dominant limitation is the inability to uniformly and controllably dehydrate GUV samples in situ. Effective dehydration in our experiments is achieved using vacuum-assisted drying, which cannot be readily implemented during live microscopy. Simple air-drying under the microscope results in poorly controlled and spatially heterogeneous drying, and the rate of water loss—which is known to influence membrane deformation and protein organization—would be difficult to define or reproduce.

In the experiments reported in the main figures, GUVs were subjected to a single, well-defined dehydration–rehydration cycle to enable clear interpretation of CAHS12-dependent effects. We also tested repeated dehydration–rehydration cycles and found that the GUVs could undergo at least three consecutive cycles, as demonstrated by representative fluorescence microscopy images in **Supplementary Fig. 3A**.

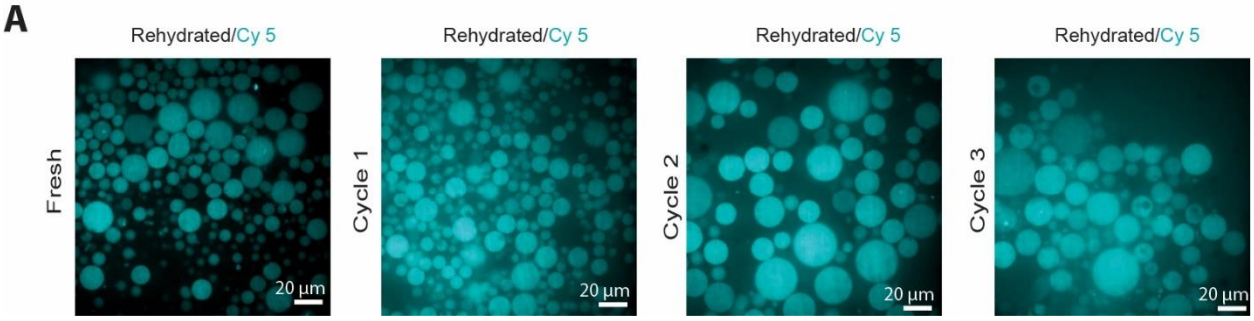

Supplementary Fig. 3A. Representative fluorescence microscopy images of GUVs after repeated dehydration–rehydration cycles. *Representative fluorescence microscopy images of GUVs following three consecutive dehydration–rehydration cycles. After each dehydration step (vacuum desiccation at ~31 mbar for ≥12 h), samples were rehydrated by adding ultrapure water and incubated at room temperature for 10 min to allow complete rehydration before imaging or initiation of the subsequent cycle. Vesicle morphology and integrity were assessed after each rehydration. Some vesicles appeared larger after the first dehydration-rehydration cycle, for reasons we do not fully understand.*

2. In Figure 1I, the three data points for the three proteins at 0 mM concentration, and the point at 0 on the protein-free curve, should represent identical conditions. Why is there a significant variation in the measured tension among these four points?

Response: We thank the reviewer for raising this point and appreciate the opportunity to clarify. Importantly, there is no actual difference among the four data points at 0 mM protein. All measurements at 0 mM correspond to the same condition and yielded an interfacial tension of ~26.5 mN/m. The apparent discrepancy arises from the fact that we measured interfacial tension at very low protein concentrations (e.g., 10 µM) in close proximity to 0 µM. When the full concentration range is plotted, these nearby low-concentration data points can visually give the impression that the baseline (0 mM) values differ among samples, even though they are identical. To address this potential confusion, we have now added a zoomed-in view of the 0–100 µM range to **Supplementary Fig. 8D**, which clearly shows that all four samples share the same baseline interfacial tension at 0 mM.

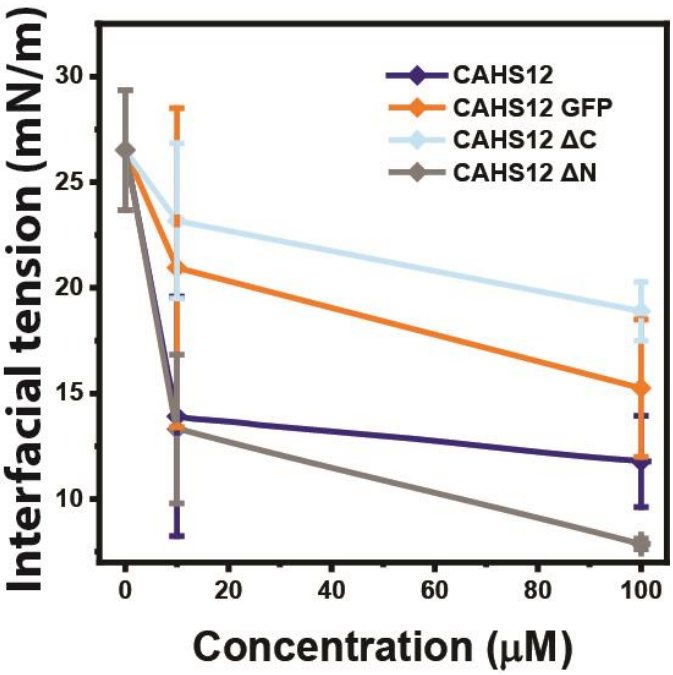

Supplementary Fig. 8. (**D**) IFT as a function of concentration for CAHS12, CAHS12 GFP, CAHS12 ΔC, and CAHS12 ΔN.

3. In the long-term CFE preservation experiment, a crucial quantitative control is missing. How much activity, if any, is retained by the CFE system in solution (not encapsulated within GUVs) under the same desiccation conditions? This would more clearly delineate the respective contributions of GUV encapsulation versus CAHS12 protection.

Response: We thank the reviewer for this important suggestion. To directly address this point, we have systematically compared the activity retention of bulk (non-encapsulated) CFE systems with and without CAHS12 following dehydration and dry storage for different durations. These results are now presented in **Supplementary Fig. 25F**. We find that bulk CFE reactions rapidly lose activity upon dehydration, and that the addition of CAHS12 in bulk solution provides only limited protection over time.

In contrast, when the same CFE system is encapsulated within GUVs, CAHS12 enables substantial recovery of translational activity after long-term dry storage, as shown in **Fig. 4**. Although the majority of the encapsulated volume is not in direct contact with the membrane, encapsulation nonetheless imposes a confined and heterogeneous environment that differs fundamentally from bulk solution. Such compartmentalization may influence local concentration profiles, drying and rehydration kinetics, or the spatial organization of macromolecular components during dehydration, thereby enhancing the protective effects of CAHS12.

Importantly, our data indicate that CAHS12-mediated protection is strongly context-dependent: while CAHS12 alone provides only modest stabilization in bulk solution, its protective capacity is markedly enhanced within a compartmentalized GUV environment. We note that the precise physical and molecular mechanisms underlying this synergy remain an important topic for future investigation.

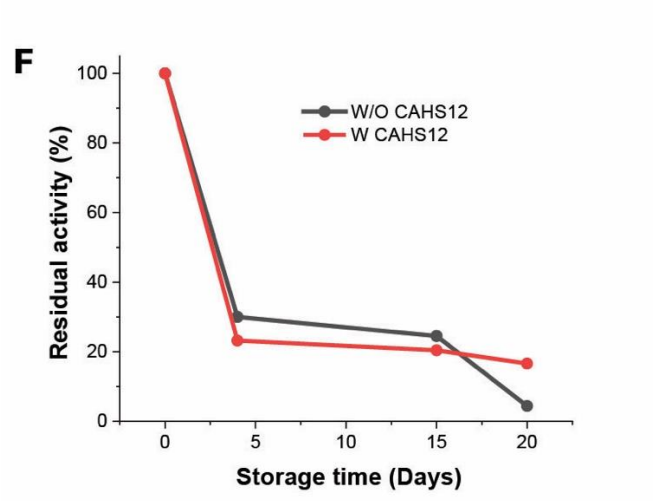

Supplementary Fig. 25. (**F**) **Activity retention of bulk cell-free expression (CFE) systems after dry storage.** Bulk (non-encapsulated) CFE reactions with or without CAHS12 were dehydrated and stored under identical conditions for different durations, followed by rehydration and assessment of translational activity via mCherry expression. Activity retention is reported relative to freshly prepared, non-dried bulk CFE controls.

4. Regarding the definition of "survival rate," how is the survival rate of GUVs precisely defined? Is it based solely on morphological integrity, content retention, or a combination of both?

Response: We thank the reviewer for requesting clarification. In this study, the “survival rate” of GUVs is defined based on a combination of morphological integrity and content retention after dehydration–rehydration, rather than morphology alone. Specifically, GUVs were scored as “surviving” if, after rehydration, they retained a closed, vesicular morphology (i.e., no collapse or rupture), and preserved internal fluorescent cargo (e.g., Cy5), indicating minimal leakage during dehydration and rehydration.

Vesicles that exhibited membrane collapse, rupture, or complete loss of internal fluorescence were classified as non-surviving. In response to a comment by another reviewer, we have revised the figure legends and Methods section to explicitly state this operational definition and avoid

ambiguity associated with the term “survival,” which does not imply biological viability but rather structural and functional preservation of synthetic compartments.

5. Molecular simulations strongly suggest that CAHS12 forms a filamentous network upon dehydration. Is there any more direct experimental evidence, or reported by literature?

Response: We appreciate the reviewer’s interest in direct experimental support for the filamentous assemblies suggested by molecular simulations. Our simulations do indeed predict that CAHS12 undergoes dehydration-induced self-association into an extended, filamentous network, which mechanically reinforces the vesicle interior.

Experimentally, while we do not directly visualize individual filaments at molecular resolution, we do note one observation that provides indirect support: fluorescence microscopy of dehydrated GUVs reveals the formation of dense, interconnected CAHS12 assemblies within the vesicle lumen, which reversibly disassemble upon rehydration (**Fig. 1G**).

In addition, prior studies on CAHS-family proteins have reported dehydration- or stress-induced formation of filamentous or gel-like assemblies in cells and in vitro[1,5,9], supporting the idea that CAHS proteins can form extended, stress-responsive networks. We have now included several references supporting the formation of filamentous networks of CAHS-family proteins. We view the simulations as providing molecular-level insight into a dehydration-induced assembly process that is consistent with, and supported by, our experimental observations and prior literature, while acknowledging that higher-resolution structural characterization will be an important direction for future work.

Reference

1. Tanaka, A. *et al.* Stress-dependent cell stiffening by tardigrade tolerance proteins that reversibly form a filamentous network and gel. *PLoS Biol.* **20**, e3001780 (2022).
2. Boothby, T. C. *et al.* Tardigrades Use Intrinsically Disordered Proteins to Survive Desiccation. *Mol. Cell* **65**, 975-984.e5 (2017).
3. Crowe, J. H. Anhydrobiosis: An Unsolved Problem with Applications in Human Welfare. *Subcell. Biochem.* **71**, 263–280 (2015).
4. Boothby, T. C. Water content influences the vitrified properties of CAHS proteins. *Molecular Cell* vol. 81 411–413 Preprint at https://doi.org/10.1016/j.molcel.2020.12.009 (2021).

5. Sanchez-Martinez, S. *et al.* Labile assembly of a tardigrade protein induces biostasis. *Protein Science* **33**, e4941 (2024).

6. Yagi-Utsumi, M. *et al.* Desiccation-induced fibrous condensation of CAHS protein from an anhydrobiotic tardigrade. *Sci. Rep.* **11**, (2021).

7. Malki, A. *et al.* Intrinsically Disordered Tardigrade Proteins Self-Assemble into Fibrous Gels in Response to Environmental Stress. *Angewandte Chemie - International Edition* **61**, e202109961 (2022).

8. Piszkiewicz, S. *et al.* Protecting activity of desiccated enzymes. *Protein Science* **28**, 941–951 (2019).

9. Sanchez-Martinez, S., Ramirez, J. F., Meese, E. K., Childs, C. A. & Boothby, T. C. The tardigrade protein CAHS D interacts with, but does not retain, water in hydrated and desiccated systems. *Sci. Rep.* **13**, (2023).

10. Biswas, S. *et al.* Helicity of a tardigrade disordered protein contributes to its protective function during desiccation. *Protein Science* **33**, e4872 (2024).

11. Boothby, T. C. *et al.* Tardigrades Use Intrinsically Disordered Proteins to Survive Desiccation. *Mol. Cell* **65**, 975-984.e5 (2017).

12. Nguyen, K. *et al.* A phase transition modulates the protective function of a tardigrade disordered protein during desiccation. *Protein Science* **34**, (2025).

13. Eicher, J. E. *et al.* Secondary structure and stability of a gel-forming tardigrade desiccation-tolerance protein. *Protein Science* **31**, e4495 (2022).

14. Bonomi, M. *et al.* Promoting transparency and reproducibility in enhanced molecular simulations. *Nature Methods 2019 16:8* **16**, 670–673 (2019).

15. WHAM – Grossfield Lab. http://membrane.urmc.rochester.edu/wordpress/?page_id=126.

16. Humphrey, W., Dalke, A. & Schulten, K. VMD: visual molecular dynamics. *Elsevier* **14**, 33–38 (1996).

17. Navarro-Retamal, C. *et al.* Folding and Lipid Composition Determine Membrane Interaction of the Disordered Protein COR15A. *Biophys. J.* **115**, 968–980 (2018).

18. Hernández-Sánchez, I. E. *et al.* LEAfing through literature: late embryogenesis abundant proteins coming of age—achievements and perspectives. *J. Exp. Bot.* **73**, 6525–6546 (2022).

19. Hesgrove, C. & Boothby, T. C. The biology of tardigrade disordered proteins in extreme stress tolerance. *Cell Communication and Signaling* **18**, 1–15 (2020).

20. Bino, T., Goto, Y., Maryu, G., Arakawa, K. & Aoki, K. Possible roles of CAHS proteins from Tardigrade in osmotic stress tolerance in mammalian cells. *Cell Struct. Funct.* **49**, 123–133 (2024).

21. Zarubin, M. *et al.* Structural study of the intrinsically disordered tardigrade damage suppressor protein (Dsup) and its complex with DNA. *Scientific Reports 2024 14:1* **14**, 22910- (2024).

22. Yamaguchi, A. *et al.* Two Novel Heat-Soluble Protein Families Abundantly Expressed in an Anhydrobiotic Tardigrade. *PLoS One* **7**, e44209 (2012).

23. Ibarboure, E., Fauquignon, M. & Le Meins, J. F. Obtention of giant unilamellar hybrid vesicles by electroformation and measurement of their mechanical properties by micropipette aspiration. *hal.scienceE Ibarboure, M Fauquignon, JF Le MeinsJournal of visualized experiments: JoVE, 2020•hal.science* **2020**, (2019).

24. Dimova, R. & Marques, C. *The Giant Vesicle Book*. *The Giant Vesicle Book* (CRC Press, 2019). doi:10.1201/9781315152516.